

A Systematic Investigation of Feature-Based Visual Learning: Mechanisms and Application

Zhiyan Wang, Sc.M.

Brown University

Dissertation

Submitted in partial fulfillment of the requirements for the Degree of Doctor of
Philosophy in the Department of Cognitive, Linguistic, and Psychological Sciences at
Brown University

PROVIDENCE, RHODE ISLAND

MAY 2021

© Copyright 2021 by Zhiyan Wang

NOTE: The year of copyright is the same as the year the degree is conferred.

This dissertation by Zhiyan Wang is accepted in its present form by the Department of
Cognitive, Linguistic and Psychological Sciences as satisfying the dissertation
requirement for the degree of Doctor of Philosophy.

Date _____

Dr. Takeo Watanabe, Advisor

Recommended to the Graduate Council

Date _____

Dr. Michael J. Frank, Reader

Date _____

Dr. Yuka Sasaki, Reader

Approved by the Graduate Council

Date _____

Andrew G. Campell, Dean of the Graduate School

Curriculum Vitae

Education

- 2016- **Ph.D. candidate in Psychology**
Cognitive and Perceptual Learning Lab
Department of Cognitive, Linguistic and Psychological Sciences
Brown University
Advisor: Takeo Watanabe
- 2016-2018 **M.A. in Psychology**
Department of Cognitive, Linguistic and Psychological Sciences
Brown University
Master Thesis: The mechanisms of visual perceptual learning
- 2012-2016 **B.S. in Psychology**
Department of Cognitive and Psychological Sciences
Peking University, China
Thesis: Lateral Interactions and Grouping in Adaptation

Professional Experience

- 2019 – 2020 **Trainee for T32 Training Grant Interactionist Cognitive Neuroscience**
Robert J. & Nancy D. Carney Institute for Brain Science
Brown University
PIs: Takeo Watanabe, Yuka Sasaki, Michael Frank, David Badre, Christopher Moore
- 2013 - 2016 **Research Assistant in Accurate Vision Lab**
Department of Cognitive and Psychological Sciences
Peking University, China
PI: Cong Yu
- 2015.7 - 2015.9 **Visiting Research Assistant in Cognitive and Perceptual Learning Lab**
Department of Cognitive, Linguistic and Psychological Sciences
Brown University
PI: Takeo Watanabe
- 2014 - 2015 **National Undergraduate Innovative Research Program**
Department of Cognitive and Psychological Sciences
Peking University, China
Project: Feature-based attention and its influence on the transfer of visual perceptual learning

Publications

Peer-reviewed journal article

Tan Q*, **Wang Z.***, Sasaki Y., Watanabe T. (2019). Category-induced transfer of visual perceptual learning. *Current Biology*. 29 (8): 1374-1378. (*equal contributions)
Tamaki, M., **Wang, Z.**, Watanabe, T., & Sasaki, Y. (2019). Trained-feature-specific offline learning by sleep in an orientation detection task. *Journal of vision*, 19(12), 12-12.
Tamaki, M., **Wang, Z.**, Barnes-Diana, T., Guo, D., Berard, A. V., Walsh, E., ... & Sasaki, Y. (2020). Complementary contributions of non-REM and REM sleep to visual learning. *Nature Neuroscience*, 23(9), 1150-1156.

Book Chapters

Wang, Z., Sasaki, Y., Watanabe, T. (2021). Chapter 4: fMRI neurofeedback for perception and attention. *fMRI Neurofeedback*. Elsevier.

Preprints and journal articles under review

Wang Z., Kim D., Pedroncelli G., Sasaki Y., Watanabe T.(preprint) Reward evokes visual perceptual learning following reinforcement learning rules.

doi: <https://doi.org/10.1101/760017>

Wang, Z., Tamaki, M., Shibata, K., Worden, M. S., Yamada, T., Sasaki, Y., ... & Watanabe, T. (preprint). Visual perceptual learning of a primitive feature in human V1/V2 as a result of unconscious processing, revealed by Decoded fMRI Neurofeedback (DecNef). Under review.

In preparation

Wang Z., Kim D., Sasaki Y., Watanabe T. (in preparation). Different degrees of generalization following reward and alertness induced learning.

Wang Z., Tan Q., Frank S., Sheinberg D., Philips K., Sasaki Y., Watanabe T. (in preparation). Visual perceptual learning of faces induces global changes in body dysmorphic disorder patients.

Conference Presentations

Wang Z., Kim D., Sasaki Y., Watanabe T. (2017) Reward may explain how reward evokes visual perceptual learning. Poster presentation at *2017 Vision Science Society Annual Meeting*, Tampa, Florida / Poster presentation at 'Atoms, Axons, and Asteroids: Big Data in STEM' – *Young Scholar Conference 2017*, Providence, Rhode Island

Wang Z., Tamaki M., Shibata K., Worden M., Sasaki Y., Watanabe T. (2018) Feature-based plasticity revealed by decoded fMRI neural feedback (DecNef). Poster presentation at *2018 Vision Science Society Annual Meeting*, Tampa, Florida.

Wang Z., Kim D., Hu C., Sasaki Y., Watanabe T. (2018) Reward may evoke visual perceptual learning following reinforcement learning rules. Poster presentation at *2018 Society for Neuroscience Annual Meeting*, San Diego, California.

Tamaki, M., **Wang, Z.**, Barnes-Diana, T., Yamada, T., Walsh, E. G., Watanabe, T., & Sasaki, Y. (2019). Different but complementary roles of NREM and REM sleep in facilitation of visual perceptual learning associated with neurotransmitters changes

revealed by magnetic resonance spectroscopy. Poster presentation at 2019 *Vision Science Society Annual Meeting*, Tampa, Florida.

Wang, Z., Kim, D., Pedroncelli, G., Sasaki, Y., & Watanabe, T. (2020). Alertness-induced transfer of visual perceptual learning to untrained orientations and eye, which is induced by neither reward nor attention. Poster presentation at 2020 *Virtual Vision Science Society Annual Meeting*, Tampa, Florida.

Yamada, T., Tamaki, M., **Wang, Z.**, Watanabe, T., & Sasaki, Y. (2020). Interactions of reward and sleep can be harmful to presleep visual perceptual learning by rendering the learning more vulnerable to interference or catastrophic forgetting. Poster presentation at 2020 *Virtual Vision Science Society Annual Meeting*, Tampa, Florida.

Wang Z., Tan Q., Frank S., Sheinberg D., Philips K., Sasaki Y., Watanabe T. (2021). Substantial changes in global brain processing related to face perception in body dysmorphic disorder patients by training on low spatial frequency components in faces. Talk presentation at 2021 *Virtual Vision Science Society Annual Meeting*, Tampa, Florida.

Honors and Awards

2019-2020	Trainee of T32 Training Grant Interactionist Cognitive Neuroscience
2016-2017	Brown University Graduate Student Fellowship
2015-2016	Peking University Wusi Fellowship, China
2014-2015	Peking University Award for Good Academic Standing, China
2014-2015	National Innovation Award for Undergraduate Research, China

Services

2017-2018	Organizer, Perception and Action Seminar Series Department of Cognitive, Linguistic and Psychological Sciences Brown University
-----------	--

Certificates

2018	Sheridan Teaching Certificate – Level 2 (Course Design)
2017	Sheridan Teaching Certificate – Level 1
2020	Brown University MRI Research Facility – Level 3

Teaching

2017 Fall	Teaching assistant for CLPS 0900 Statistical Methods
2018 Spring	Teaching assistant for CLPS 0900 Statistical Methods
2018 Fall	Teaching assistant for CLPS 0120 Introduction to Sleep
2019 Spring of Happiness	Teaching assistant for CLPS 0710 The Psychology and Philosophy

Mentoring

Undergraduate	Chun Hu
Master/ Intern	Giorgia Pedroncelli

Preface and Acknowledgement

Visual perceptual learning is studying the enhancement of visual performance after visual experiences. The dissertation aims to illustrate the mechanisms of feature-based plasticity in association with visual perceptual learning. The dissertation illustrated three challenges in feature-based visual learning and plasticity with decoded fMRI neurofeedback, psychophysics as well as computational modeling.

During my Ph.D while completing this dissertation work, I received enormous help and support from my advisors and my dissertation committee, Professor Takeo Watanabe, Professor Yuka Sasaki and Professor Michael Frank. I would also like to thank my advisor Takeo Watanabe for providing me with enormous opportunities to pursue my interest and to explore new methods and topics in visual perceptual learning. I would also like to express my gratitude for my lab members who offered great suggestions for the dissertation work along my Ph.D years. I also really appreciated our invaluable discussions in- and-out of the lab context. Particularly, I would like to thank Dr. Masako Tamaki for guiding me through my initial years of Ph.D and offering endless help.

I would not have succeeded without the help from my family and friends. I would like to thank my friends for providing support and for helping me maintaining a balanced life during Ph.D, especially our little weekend dining and boardgame group and my tennis group. I would also like to thank my families, my mom and dad and my partner Sebastian, for always being with me and offering unconditional love and support.

Lastly, I would like to acknowledge the Carney Institute for Brain Science for supporting my dissertation work with the T32 ICON training grant.

Table of Contents

GENERAL INTRODUCTION.....	1
DISSERTATION AIMS.....	7
AIM 1: WHETHER FEATURE-BASED PLASTICITY CAN OCCUR INDEPENDENTLY AND WHERE IN THE BRAIN IT CAN OCCUR.....	7
AIM 2: WHAT FACTORS ARE INVOLVED IN THE DEVELOPMENT OF FEATURE-BASED PLASTICITY.....	8
AIM 3: HIGHER LEVEL VISUAL FEATURES: PLASTICITY AND APPLICATION	9
GENERAL METHODS	11
GENERAL ANALYSIS	14
AIM 1: WHETHER FEATURE-BASED PLASTICITY CAN OCCUR INDEPENDENTLY AND WHERE IN THE BRAIN IT CAN OCCUR	16
INTRODUCTION	16
EXPERIMENT 1.....	19
EXPERIMENT 2.....	30
DISCUSSION AND CONCLUSION	32
AIM 2: WHAT FACTORS ARE INVOLVED IN THE DEVELOPMENT OF FEATURE-BASED PLASTICITY	35
INTRODUCTION	35
EXPERIMENT 3.....	37
EXPERIMENT 4.....	43
EXPERIMENT 5: MODEL FITTING.....	45
DISCUSSION AND CONCLUSION	52
AIM 3: HIGHER LEVEL VISUAL FEATURES: PLASTICITY AND APPLICATION	56
INTRODUCTION	56
EXPERIMENT 6.....	59
DISCUSSION AND CONCLUSION	73
GENERAL DISCUSSION AND CONCLUSIONS.....	78
REFERENCES	81

List of Figures and Tables

FIGURE 1. ILLUSTRATION OF VISUAL STIMULI USED IN VISUAL PERCEPTUAL LEARNING. A) AN ORIENTATION STIMULUS CONSISTED OF A SINUSOIDAL GRATING OVERLAID WITH GAUSSIAN NOISE. THE ORIENTATION OF THE GRATING AND THE SIGNAL-TO-NOISE RATIO ARE THE PARAMETERS THAT ARE USUALLY MANIPULATED IN EXPERIMENTS. B) A MOTION STIMULUS CONSISTED OF RANDOMLY MOVING DOTS. A CERTAIN PERCENTAGE OF THE DOTS MOVE IN THE SAME DIRECTION.	2
FIGURE 2. TASK- AND FEATURE-BASED PLASTICITY. THE FIGURE ILLUSTRATES THE RELATIONSHIP BETWEEN DIFFERENT TYPES OF LEARNING AND THE TWO TYPES OF PLASTICITY. TASK-RELEVANT PERCEPTUAL LEARNING CONSISTS OF BOTH TYPES OF PLASTICITY, WHEREAS TASK-IRRELEVANT PERCEPTUAL LEARNING CONSISTS OF ONLY FEATURE-BASED PLASTICITY. THIS FIGURE IS A MODIFIED VERSION OF WATANABE & SASAKI, 2015.....	6
FIGURE 3 HYPOTHESIS FOR EXPERIMENT 1. A) ONLY FEATURE-BASED PLASTICITY IS INDUCED WITH DECNEF IN V1/V2. B) BOTH FEATURE-BASED AND TASK-BASED PLASTICITY IS INDUCED WITH DECNEF. C) ONLY TASK-BASED PLASTICITY IS INDUCED WITH DECNEF.	18
FIGURE 4. EXPERIMENT 1 TIMELINE.	19
FIGURE 5 STIMULI IN EXPERIMENT 1. A) SEKULER DISPLAY. THE GLOBAL MOTION IS SHOWN AS THE RED ARROW, WHICH IS THE TEMPORAL AND SPATIAL AVERAGE OF THE LOCAL MOTION SIGNALS. B) ILLUSTRATION OF THE GLOBAL AND LOCAL MOTION DIRECTIONS USED IN SEKULER MOTION. THE LOCAL MOTION RANGES WERE IN BLUE, WHILE THE GLOBAL MOTION DIRECTION WAS SHOWN IN RED. C) COHERENT MOTIONS THAT WERE PRESENTED DURING PRE- AND POSTTESTS CONSISTED OF THE GLOBAL MOTIONS (RED), LOCAL MOTIONS (BLUE), AND OTHER MOTION DIRECTIONS (BROWN).	20
FIGURE 6 PERFORMANCE IMPROVEMENT ON THE MOTION DISCRIMINATION TASK. A) MEAN (+/- SEM) IMPROVEMENT IN THE TRAINED MOTION RANGE. IMPROVEMENT WAS FOUND IN THE TRAINED LOCAL MOTION RANGES. B) MEAN (+/- SEM) IMPROVEMENT IN THE TRAINED MOTION RANGE. NO SIGNIFICANT IMPROVEMENT WAS FOUND. 0 DEG REPRESENTS THE GLOBAL MOTION DIRECTION. THE RED LINE INDICATES THE FITTED CURVE OF THE TUNING FUNCTION. THE SHADED AREA CORRESPONDS TO THE LOCAL MOTION RANGES.	28
FIGURE 7 MEAN (+/- SEM) IMPROVEMENT FOR THE TRAINED AND THE UNTRAINED LOCAL MOTION RANGES. THERE WAS SIGNIFICANT IMPROVEMENT ONLY IN THE TRAINED LOCAL MOTION RANGES. * $p < .05$	29
FIGURE 8. MEAN FISHER-TRANSFORMED CORRELATION COEFFICIENT BETWEEN THE INDUCED PATTERN AND THE RECONSTRUCTED SCORE IN ROIS. V1/V2 (TARGET ROI) WERE SHOWN IN RED, AND THE OTHER CONTROL ROIS WERE SHOWN IN BLACK. ONLY THE ACTIVATION PATTERN IN V1/V2 (RED) CAN SIGNIFICANTLY RECONSTRUCT THE ESTIMATED SCORES OF THE V1/V2 ACTIVATION PATTERN DURING THE NEUROFEEDBACK STAGE [$z = 8.171, p = 0.000$]. *** $p < .001$	30
FIGURE 9. D-PRIME IMPROVEMENT FOR LOCAL MOTION RANGES IN EXPERIMENT 2. THERE WAS NO SIGNIFICANT IMPROVEMENT FOR THE CLOCKWISE OR THE COUNTERCLOCKWISE LOCAL MOTION RANGES.	32
FIGURE 10. PROCEDURE FOR EXPERIMENT 3 AND EXPERIMENT 4. A) ORIENTATION DETECTION TASK IN THE PRE- AND POSTTEST STAGES. SUBJECTS WERE REQUESTED TO DECIDE WHICH ORIENTATION WAS PRESENTED WHEN THE FIXATION POINT TURNED RED. B) THE ILLUSTRATION OF THE HAPLOSCOPE AND THE WATER DELIVERY DEVICE. C) CFS PARADIGM IN THE TRAINING SESSIONS FOR EXPERIMENT 3. WATER REWARD WAS PAIRED WITH THE TRAINED ORIENTATION IN THE TRAINED EYE. D) CFS PARADIGM IN THE TRAINING SESSIONS FOR EXPERIMENT 4. AROUSAL SOUND WAS PRESENTED IN ASSOCIATION WITH THE TRAINED ORIENTATION. PART OF THE FIGURE WAS ALSO SHOWN IN THE PREPRINT (Z. WANG, KIM, PEDRONCELLI, SASAKI, & WATANABE, 2019).....	40
FIGURE 11. PERCENT CORRECT CHANGE FOR THE 'REWARD BEFORE' (A) AND THE 'REWARD AFTER' (B) GROUP. THE PERCENT CORRECT WAS SHOWN IN DIFFERENT PANELS. THE LINE INDICATES THE MEAN AND THE SEM IS SHOWN IN THE RIBBON. BLUE REPRESENTS THE PRETEST, AND RED REPRESENTS THE POSTTEST. SIGNIFICANT IMPROVEMENT WAS ONLY FOUND FOR THE REWARD AFTER CONDITION FOR THE PAIRED ORIENTATION IN THE TRAINED EYE. * $p < .05$. ** $p < .01$	42
FIGURE 12. PERCENT CORRECT CHANGE FOR THE 'AROUSAL BEFORE' (A) AND THE 'AROUSAL AFTER' (B) GROUP. THE PERCENT CORRECT WAS SHOWN IN DIFFERENT PANELS. THE LINE INDICATES THE MEAN, AND THE SEM IS SHOWN IN THE RIBBON. BLUE REPRESENTS THE PRETEST, AND RED REPRESENTS THE POSTTEST. SIGNIFICANT IMPROVEMENT WAS FOUND IN BOTH GROUPS. * $p < .05$	45
FIGURE 13. A NORMALIZATION MODEL OF REWARD AND AROUSAL. THE MODEL CONSISTED OF STIMULUS DRIVE, AROUSAL, AND REWARD FIELD. THE THREE EFFECTS WERE MULTIPLIED TO CONSTRUCT THE OVERALL EXCITATION, WHICH WAS THE NOMINATOR OF THE MODEL. THE NOMINATOR WAS CONVOLUTED WITH THE INHIBITORY FIELD TO GENERATE THE	

MODEL'S SUPPRESSIVE DRIVE, WHICH WAS THE DENOMINATOR OF THE MODEL. THE POPULATION RESPONSE WAS ACQUIRED BY THE OVERALL EXCITATION DIVIDED (NORMALIZED) BY THE SUPPRESSIVE DRIVE.....	47
FIGURE 14. MODEL FITTING FOR THE 'AROUSAL BEFORE' CONDITION. THE GOODNESS-OF-FIT WAS 0.82. A) COMPARISON BETWEEN MODEL AND PSYCHOPHYSICAL DATA. THE MODEL WAS SHOWN IN LINES, AND THE PSYCHOPHYSICAL DATA WAS SHOWN IN DOTS WITH ERROR BARS REPRESENTING THE SEM. B) SCHEMATIC ILLUSTRATION OF MODEL PARAMETERS. 0 INDICATED THE TRAINED ORIENTATION AND SPATIAL LOCATION.	48
FIGURE 15. MODEL FITTING FOR THE 'AROUSAL AFTER' CONDITION. THE GOODNESS-OF-FIT WAS 0.94. A) COMPARISON BETWEEN MODEL AND PSYCHOPHYSICAL DATA. THE MODEL WAS SHOWN IN LINES AND THE PSYCHOPHYSICAL DATA WAS SHOWN IN DOTS WITH ERROR BARS REPRESENTING THE SEM. B) SCHEMATIC ILLUSTRATION OF MODEL PARAMETERS. 0 INDICATED THE TRAINED ORIENTATION AND SPATIAL LOCATION.	49
FIGURE 16. MODEL FITTING FOR THE 'REWARD BEFORE' CONDITION. THE GOODNESS-OF-FIT WAS 0.77. A) COMPARISON BETWEEN MODEL AND PSYCHOPHYSICAL DATA. THE MODEL WAS SHOWN IN LINES AND THE PSYCHOPHYSICAL DATA WAS SHOWN IN DOTS WITH ERROR BARS REPRESENTING THE SEM. B) SCHEMATIC ILLUSTRATION OF MODEL PARAMETERS. 0 INDICATED THE TRAINED ORIENTATION AND SPATIAL LOCATION.	50
FIGURE 17. MODEL FITTING FOR THE 'REWARD AFTER' CONDITION. THE GOODNESS-OF-FIT WAS 0.81. A) COMPARISON BETWEEN MODEL AND PSYCHOPHYSICAL DATA. THE MODEL WAS SHOWN IN LINES, AND THE PSYCHOPHYSICAL DATA WAS SHOWN IN DOTS WITH ERROR BARS REPRESENTING THE SEM. B) SCHEMATIC ILLUSTRATION OF MODEL PARAMETERS. 0 INDICATED THE TRAINED ORIENTATION AND SPATIAL LOCATION.	52
FIGURE 18. METHODS FOR EXPERIMENT 6. A) ILLUSTRATION OF FOUR TYPES OF VISUAL STIMULI USED DURING SENSITIVITY MEASUREMENT, PRE- AND POSTTEST STAGES. THE STIMULI INCLUDE LOW SPATIAL FREQUENCY (LSF) AND HIGH SPATIAL FREQUENCY (HSF) FACE AND LOW AND HIGH SPATIAL FREQUENCY HOUSE. B) ONE TRIAL IN THE 2IFC TASK. C) EXPERIMENT TIMELINE. THE RED BOX INDICATES SESSIONS THAT WERE CONDUCTED IN THE MRI. D) EXAMPLE FOR FUNCTIONAL CONNECTIVITY. THE FIGURE SHOWS THE TIME COURSE OF RESIDUALS USED IN FUNCTIONAL CONNECTIVITY FROM THE LEFT AND RIGHT FFA.....	60
FIGURE 19. PERFORMANCE IMPROVEMENT FOR THE BDD (N = 9) AND THE CONTROL GROUP (N=10). BOTH GROUPS SHOWED SIGNIFICANT IMPROVEMENT ONLY FOR THE LOW SPATIAL FREQUENCY FACE, WHICH WAS THE TRAINED CONDITION. + P<.05 BEFORE MULTIPLE CORRECTIONS. * P<.05 AFTER MULTIPLE CORRECTIONS.	66
FIGURE 20. BOLD ACTIVATION IN THE LEFT TEMPORAL PARIETAL JUNCTION (TPJ) FOR THE FACE (A) AND HOUSE (B) STIMULI. A) THERE WAS A SIGNIFICANT DECREASE IN THE BOLD ACTIVATION IN THE LEFT TPJ OF THE BDD SUBJECTS AFTER VPL TRAINING. THERE WAS NO CHANGE FOR THE HEALTHY CONTROL GROUP. B) THERE WAS NO CHANGE IN ASSOCIATION WITH THE HOUSE STIMULI. * P<.05.	68
FIGURE 21. BOLD LATERALIZATION INDEX IN THE FFAs FOR THE FACE (A) AND THE HOUSE (B) STIMULI. A) THE RIGHT LATERALIZATION INDEX FOR THE FACE STIMULI. THERE WAS A SIGNIFICANT INCREASE IN THE RIGHT LATERALIZATION INDEX FOR THE BDD GROUP. THERE WAS A SIGNIFICANT DECREASE IN THE RIGHT LATERALIZATION INDEX FOR THE HEALTHY CONTROL SUBJECTS. B) THERE WAS NO SIGNIFICANT CHANGE IN ASSOCIATION WITH THE HOUSE STIMULI.	70
FIGURE 22. BOLD ACTIVATION CHANGE IN THE LEFT V1 (A) AND THE RIGHT V1 (B). THERE WAS NO BOLD ACTIVATION CHANGE IN THE LEFT OR THE RIGHT V1 FOR THE BDD OR THE HEALTHY CONTROL SUBJECTS.	71
FIGURE 23. CORRELATION BETWEEN THE BOLD CHANGE IN RIGHT LATERALIZATION INDEX AND THE PERFORMANCE IMPROVEMENT IN THE BDD GROUP.....	71
FIGURE 24. FUNCTIONAL CONNECTIVITY CHANGE. A) FISHER-TRANSFORMED CORRELATION COEFFICIENT BETWEEN THE LEFT TPJ AND THE RIGHT OFA. THERE WAS A SIGNIFICANT INCREASE IN THE CORRELATION COEFFICIENT IN THE BDD GROUP AFTER TRAINING. B) FISHER-TRANSFORMED CORRELATION COEFFICIENT BETWEEN THE LEFT AND RIGHT FFA. THERE WAS A SIGNIFICANT DECREASE IN BILATERAL CONNECTIVITY IN THE FFA FOR THE BDD GROUP . THERE WAS SIGNIFICANT INCREASE IN BILATERAL CONNECTIVITY IN THE FFA FOR THE HEALTHY CONTROL GROUP. ** P<.01. * P<.05.....	73
TABLE 1. REPORTED STRATEGIES DURING THE NEUROFEEDBACK STAGE.....	25

Abstract of A Systematic Investigation of Feature-Based Visual Learning: Mechanisms and Application, by Zhiyan Wang, Ph.D., Brown University, May 2021.

Visual perceptual learning is defined as visual performance improvement after visual perceptual experiences. It is controversial how changes in association with feature representation change, namely feature-based plasticity, occurred. In Aim 1, the dissertation investigated where do changes occur in association with feature-based plasticity. In Experiments 1 & 2, we used decoded fMRI neurofeedback to induce a pattern in V1/V2 similar to that of a Sekuler motion stimulus. The Sekuler motion consisted of both local motion directions and a global motion direction which was the summation of local motion signals. Previous psychophysical studies demonstrated that local motion directions corresponded to feature-based plasticity. Aim 1 demonstrated that after neurofeedback training in early visual areas (V1/V2), improvement was found among the local motion ranges, suggesting changes in early visual areas are associated with feature-based plasticity. In Aim 2, we performed three experiments and trained four groups of subjects: the Reward Before group, the Reward After group, the Arousal Before group, and the Arousal After group. Each group differed in the temporal order of how reward or arousal cues were paired with the trained orientation feature. Aim 2 demonstrated that reward and arousal have differential effects on feature-based plasticity. Moreover, fitting the normalization model of vision to the psychophysical data indicated an excitatory effect of arousal and an inhibitory effect of reward. In Aim 3, the dissertation demonstrated that feature-based learning of complex visual images such as faces involves feature representation changes. In Aim3, a group of BDD and healthy control subjects were trained on low spatial frequency faces to enhance holistic

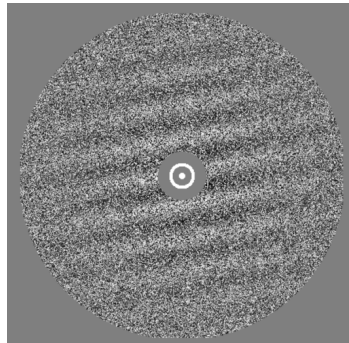
processing. The experiment showed dissociable blood-oxygen-level-dependent (BOLD) changes in body dysmorphic disorder patients and healthy control subjects consistent with their pre-training representation of holistic face processing. To conclude, our results demonstrated how feature-based visual learning occurred and can be potentially applied to clinical populations.

General Introduction

As the early pioneer Ramon y Cajal addressed in his publication to the young scientists: “Any man could, if he were so inclined, be the sculptor of his own brain”(y Cajal, 2004). To some extent, Ramon y Cajal implies that the brain is plastic enough and can be changed in response to a person’s own experience even after adulthood. We refer to this process as learning, which is ubiquitous and fundamental in animals and humans alike. The learning that occurred due to experience with the visual system after adulthood has triggered extensive interest among psychologists since the late 1800s. William James (James, 1890) and Fechner (James, 1890) conducted psychophysical tasks and observed behavioral improvement on visual discrimination tasks after training. The long-term performance improvement as a result of visual experiences is defined as visual perceptual learning and has been studied extensively as a manifestation of brain plasticity (Doshier & Lu, 2017; Sagi, 2011; Sasaki, Nanez, & Watanabe, 2010; Shibata, Sagi, & Watanabe, 2014; Watanabe & Sasaki, 2015). For instance, the accuracy of discriminating benign tissues from malignant lesions by observing a mammography image would increase dramatically with the radiologists’ years of practice (Frank et al., 2020). A novice or a naïve subject will perform poorly at this task without visual training. A professional tea merchant in China would distinguish different types and years of teas by observing tea leaves' color and shape, while a novice would fail at this task. From real-life examples, we can learn how our experiences, namely, training, can ‘sculpt’ our brains.

In a lab environment, visual perceptual learning is usually investigated with simplified stimuli representing a type of visual feature. As shown in Figure 1, oriented gratings (Figure 1A) or moving dots (Figure 1B) are typically used to test the performance of orientation discrimination or motion discrimination. The orientation and signal-to-noise ratio in the grating are usually manipulated in experiments. For motion stimuli, the directions and the percentage in which the dots are collectively moving are

A)



B)

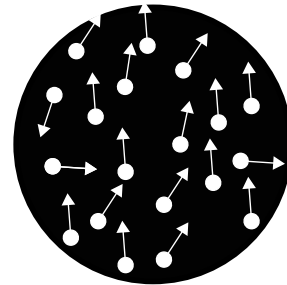


Figure 1. Illustration of visual stimuli used in visual perceptual learning. A) An orientation stimulus consisted of a sinusoidal grating overlaid with Gaussian noise. The orientation of the grating and the signal-to-noise ratio are the parameters that are usually manipulated in experiments. B) A motion stimulus consisted of randomly moving dots. A certain percentage of the dots move in the same direction.

used. It is crucial to study visual perceptual learning as a framework to understand the plasticity of the brain for the following reasons.

First and foremost, it has been well-established that the visual system develops mainly during one's critical period in infancy (Hensch, 2005a, 2005b). It is also widely accepted that the visual system will remain relatively stable after the critical period.

However, visual perceptual learning has shown that even the visual system can transition from stable to plastic in response to environmental changes after the system has developed sophisticatedly. Therefore, the changes of visual systems might serve as a valuable tool and model to elucidate the mechanisms of learning on the whole-brain level.

Furthermore, a number of studies have applied visual perceptual learning in clinical populations, such as with amblyopia and glaucoma patients (Astle, Blighe, Webb, & McGraw, 2015; Levi, 2012; Maniglia et al., 2016; Maniglia, Soler, & Trotter, 2020; Plank et al., 2014; Polat, 2009; Polat, Ma-Naim, Belkin, & Sagi, 2004; Polat, Ma-Naim, & Spierer, 2009; Rosa, Silva, Ferreira, Murta, & Castelo-Branco, 2013; Sterkin et al., 2018). Understanding the mechanisms of visual plasticity might benefit in developing interventions to provide amelioration and restoration for clinical populations.

Finally, recent studies in visual perceptual learning have demonstrated that visual perceptual learning involves changes associated with multiple regions of the brain. The changes are related to a network of the brain including, early visual areas (H. Harris, Gliksberg, & Sagi, 2012; Karni & Sagi, 1991, 1993; Schoups, 2001; Yotsumoto, Watanabe, & Sasaki, 2008), higher-level cognitive control regions (Kahnt, Grueschow, Speck, & Haynes, 2011; Law & Gold, 2008, 2009; R. Wang, Cong, & Yu, 2013; Xiao et al., 2008; T. Zhang, Xiao, Klein, Levi, & Yu, 2010), subcortical nuclei (Yu, Zhang, Qiu, & Fang, 2016) as well as white matter connections between regions (Yotsumoto et al., 2014), etc. Therefore, visual perceptual learning studies can promote the understanding of how the visual system interacts and is influenced by other systems in the brain.

One of the major controversies in visual perceptual learning is the changes that are involved in the process. Previous studies have emphasized two aspects of changes in association with visual perceptual learning. A vast majority of studies in visual perceptual learning have demonstrated feature and location specificity. Namely, the improvement in one orientation does not transfer to other untrained orientations (Harris et al., 2012; Karni & Sagi, 1991; Schoups, 2001; Schoups, Vogels, & Orban, 1995; Shibata, Watanabe, Sasaki, & Kawato, 2011). Training in one location of the visual field does not generalize to improvement in other locations of the visual field (Jeter, Doshier, Liu, & Lu, 2010; Yotsumoto, Chang, Watanabe, & Sasaki, 2009; Yotsumoto, Sasaki, et al., 2009; Yotsumoto et al., 2008). The specificity of training has suggested that changes should have occurred in a level of visual processing that represents visual features distinctly. Therefore, these studies have indicated that visual perceptual learning involves changes in feature representation. On the other hand, some other studies have suggested that visual perceptual learning involves learning a task rule and improving on task performance (Ahissar & Hochstein, 1997, 2004; Pavlovskaya & Hochstein, 2011; R. Wang et al., 2013; R. Wang, Zhang, Klein, Levi, & Yu, 2012; Xiao et al., 2008; J.-Y. Zhang et al., 2008; J.-Y. Zhang et al., 2010; T. Zhang et al., 2010). Under these circumstances, visual perceptual learning occurred due to repetitive processing of a task and improving on the rules of a task instead of changes in the feature representation. A dual-plasticity model has been proposed recently to reconcile the controversies about the changes in association with visual perceptual learning (Watanabe & Sasaki, 2015). This model has summarized that visual perceptual learning involves changes in feature representation, termed feature-based plasticity, and changes in task processing termed

task-based plasticity. Although the model has suggested a comprehensive theory to explain the mechanisms of visual plasticity, there is no clear evidence that indicates that feature-based plasticity can occur independently of task-based plasticity. Moreover, the mechanisms of feature-based plasticity also remain elusive. It is also unclear whether the model expands to the learning of a natural and complex visual stimulus.

One important factor has challenged the investigation of feature-based plasticity. It is not entirely clear whether we can separate tasks and features in a visual training experiment. Behavioral improvement on a visual task inevitably involves both aspects. To provide evidence for feature-based plasticity alone, it is imperative for the visual training to be independent of a task. It has been suggested that there are two types of visual perceptual learning: task-relevant learning and task-irrelevant learning. Task-relevant learning refers to the training process in which the subjects perform a task relevant for the features being learning. In contrast, task-irrelevant learning refers to the process in which the subjects perform a task irrelevant to the features being trained. Task relevant learning consists of the feature- and task-based plasticity. On the other hand, task-irrelevant learning consists of only feature-based plasticity. The relationship is demonstrated in Figure 2.

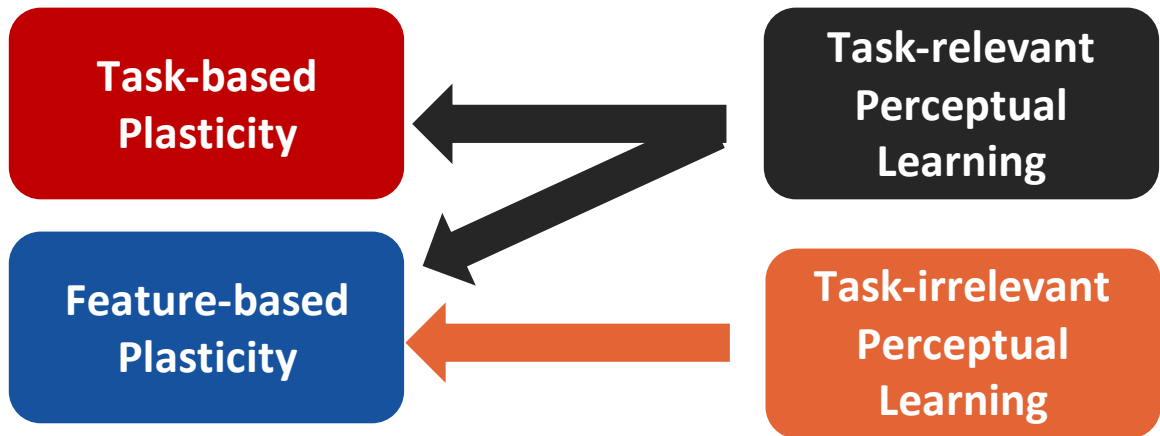


Figure 2. Task- and feature-based plasticity. The figure illustrates the relationship between different types of learning and the two types of plasticity. Task-relevant perceptual learning consists of both types of plasticity, whereas task-irrelevant perceptual learning consists of only feature-based plasticity. This figure is a modified version of Watanabe & Sasaki, 2015.

Another controversy concerning feature-based plasticity is that the models were mainly derived from the results using simple visual stimuli consisted of primitive visual features. It is unclear how features are learned with complex and natural stimuli.

Therefore, this dissertation study explores the mechanisms of feature-based plasticity through addressing the following questions mainly with task-irrelevant learning processes:

- (1) Whether feature-based plasticity can occur independently of task-based plasticity and the brain regions associated with feature-based plasticity.
- (2) What factors are involved in the development of feature-based plasticity.
- (3) The mechanisms of learning a higher-level visual feature and its application.

Dissertation Aims

Aim 1: Whether feature-based plasticity can occur independently and where in the brain it can occur.

The dissertation's first aim is to address whether feature-based plasticity can occur independently of task-based plasticity and which area in the brain does feature-based plasticity occur. Psychophysical evidence and animal studies suggest that feature-based plasticity can occur as a result of exposure to a visual feature. These experiments have shown that by exposing subjects to a visual feature (for example, motion directions) when subjects perform a different task (for example, central letter discrimination task, namely RSVP task), learning can occur to the exposed visual feature (Gutnisky, Hansen, Iliescu, & Dragoi, 2009; Pascucci, Mastropasqua, & Turatto, 2015; Seitz & Watanabe, 2003; Tsushima, Seitz, & Watanabe, 2008; Watanabe, Nanez, & Sasaki, 2001). Since under these circumstances, no behavioral task has been directed to the trained visual feature, it is plausible to assume that feature-based plasticity can occur independently of task-based plasticity. Moreover, these psychophysical studies also emphasize the specificity of learning which underpins the notion that the plasticity acquired through exposure to a task-irrelevant visual feature resides in early visual areas where primitive visual features are represented.

However, two factors precluded the conclusion that feature-based plasticity occurred and is associated with early visual areas. First of all, the psychophysical manipulation with a center task does not guarantee that attention or higher-level task processing is not involved in improving the exposed visual feature. Although the center

task is demanding, it is uncertain that subjects have never directed focused attention to the irrelevant feature. In particular, the difficulty of the central task might decrease as training proceeds. Second, the previous studies have failed to demonstrate a direct relationship between early visual areas and feature-based plasticity. The changes in early visual areas are primarily deduced from the specificity findings. Nevertheless, there is a lack of evidence from human studies to suggest a direct relationship between early visual areas and feature-based plasticity.

To address Aim 1, we conducted a study with decoded fMRI neurofeedback in a series of two experiments (Experiment 1 and 2). Decoded fMRI neurofeedback is capable of inducing a particular activation pattern specifically in a target brain region. The corresponding behavioral response will reflect the outcomes of inducing the brain activation pattern. We have the following hypotheses with regards to Aim 1.

First of all, we hypothesize that feature-based plasticity can occur independently of task-based plasticity. Second, we hypothesize that inducing visual patterns in early visual areas can result in behavioral changes corresponding to feature-based plasticity.

Aim 2: What factors are involved in the development of feature-based plasticity.

The second aim of the dissertation is to address what factors contribute to the development of feature-based plasticity. Previous psychophysical studies have shown that repetitively pairing a reward with a task-irrelevant visual stimulus can induce visual perceptual learning. Primate studies have suggested that ventral midbrain stimulation can induce visual plasticity (Arsenault & Vanduffel, 2019). These results suggest that reward is involved in the process of feature-based plasticity. Moreover, it has been suggested that Moreover, several studies also suggested that reward effectively affects feature-based

plasticity through reinforcement processes (Kahnt et al., 2011; Law & Gold, 2009; Roelfsema, van Ooyen, & Watanabe, 2010; Sasaki et al., 2010).

Reinforcement is not the only process that has been associated with reward. Several studies have suggested that reward delivery can also mediate arousal (Sara & Bouret, 2012). Animal studies have shown that arousal can improve visual perception by enhancing the signal-to-noise ratio in the visual areas (McGinley, 2020; Vinck, Batista-Brito, Knoblich, & Cardin, 2015). Arousal also affects visual perception through an enhancement of general brain states. However, it is unclear how arousal affects the processing of visual features. Furthermore, it is unclear how arousal will affect the long-term development of visual features.

Therefore, in the second aim, we addressed how reward and arousal affect the development of feature-based plasticity with two experiments (Experiment 3 and 4). Specifically, we hypothesize that 1) reward induces feature-based plasticity through reinforcement processes; 2) arousal induces feature-based plasticity through a general enhancement of brain states.

Moreover, in Aim 2, we fitted our results in Experiment 5 with a computational model to address reward and arousal effects on feature-based plasticity. In particular, the excitatory or inhibitory effects of reward and arousal on feature-based plasticity.

Aim 3: Higher level visual features: plasticity and application

The dual plasticity model states that feature-based plasticity is associated with changes in visual representation in the brain. The majority of visual studies have utilized simplified visual stimuli with primitive visual features. However, the visual stimuli in the natural environment are innately rich in visual features. The natural stimuli consist of a

combination of complex and primitive visual features. Nevertheless, it is unclear whether subjects can develop feature-based learning with natural stimuli. It is also controversial whether plasticity can be associated with changes in the brain that represent complex visual features.

Therefore, we aim to investigate the changes in association with the learning of complex visual features using natural stimuli. The results will not only provide evidence for feature-based plasticity in association with complex natural stimuli, but it will also provide implications for the application of visual perceptual learning to everyday scenarios.

In Aim 3, we trained subjects with one visual component from a complex visual stimulus in Experiment 6. We hypothesize that if feature-based learning is also associated with representation change, the improvement should be related to changes in the brain networks in which the visual component is more dominantly processed. On the other hand, if the improvement is associated with changes outside of the network representing the visual component, this will be inconsistent with our hypothesis and suggests that the learning of complex visual features does not solely depend on feature representation change, namely, feature-based plasticity.

General Methods

Subjects

A total of 71 subjects (aged 18-60) participated in the dissertation studies. In *Aim 1*, 8 subjects participated in Experiment 1 and 10 subjects participated in Experiment 2. In *Aim 2*, 18 subjects participated in Experiment 3 and 16 subjects participated in Experiment 4. In *Aim 3*, 19 subjects participated in Experiment 6. 9 out of the 19 subjects were body dysmorphic disorder patients. The other 10 subjects are healthy young adults. Healthy adult subjects were recruited from Brown University, and the patients were recruited from Rhode Island Hospital. All subjects gave written consent to the protocol approved by the institutional review board of Brown University. Subjects had normal or corrected-to-normal vision.

MRI Acquisition

Under the circumstance that MRI is performed, subjects were scanned in a 3 Tesla Siemens PRISMA scanner with a 64-channel head coil at the Magnetic Resonance Facility of Brown University. Structural images were acquired with a T1-weighted MPRAGE sequence (256 slices, voxel = 1 mm * 1 mm * 1 mm, TR = 1980 ms, TE = 3 ms, flip angle = 9°). For functional MRI scans, a gradient EPI sequence was acquired with 33 continuous slices (TR = 2 s, TE = 30 ms, flip angle = 90°, voxel = 3 mm * 3 mm * 3 mm). To align the structural images across several sessions for Experiment 1, AAScout AutoAlign (160 slices, voxel = 1.625 mm * 1.625 mm * 1.6 mm, 0 mm slice gap, TR = 3 ms, TE = 1.37 ms, flip angle = 8°) was acquired in addition.

Equipment

In Aim 1 psychophysical sessions' visual stimuli were presented on an LCD monitor (1024 X 768 resolution, 60 Hz refresh rate). The visual stimuli during MRI sessions were presented on an LCD monitor compatible with the scanner (BOLDscreen 32, Cambridge Research Systems, 1920 X 1080 resolution, 120 Hz refresh rate).

In Aim 2, the visual stimuli were presented on two identical 19'' CRT displays (1024 x 768 resolution, 120 Hz refresh rate). Subjects viewed the stimuli through a haploscope. The reward system was controlled via a water dispenser ValveLink®8.2 system manufactured by Automate Scientific, Inc.

In Aim 3, the visual stimuli were presented on a scanner-compatible LCD monitor (BOLDscreen 32, Cambridge Research Systems, 1920 X 1200 resolution, 60 Hz refresh rate). The psychophysical sessions' visual stimuli were presented on an LCD monitor (1920 X 1200 resolution, 60 Hz refresh rate).

The visual stimuli were presented with Matlab ® (MathWorks, Natick, MA) and Psychtoolbox (Brainard, 1997) controlled via Mac OS or Windows system.

General Procedure

In most cases, visual perceptual learning consisted of 3 stages: the pretest stage, the training stage, and the posttest stage. The pretest and posttest stages consisted of 1 session to measure the baseline and post-training performance. The training stages were performed for several sessions across different days. The performance was characterized as accuracy, d' or threshold. Accuracy data was calculated as the percent correct responses. D -prime was measured as $z(\text{Hit Rate}) - z(\text{False Alarm})$. D -prime was

measured to characterize for response bias. The threshold was measured with staircase procedures. Performance change was measured as percent improvement change as a result of training, which was calculated as $(\text{posttest} - \text{pretest}) / \text{pretest} \times 100\%$.

General Analysis

fMRI Preprocess

fMRI preprocess was conducted with Freesurfer (Fischl, 2012) and FsFast toolbox across the experiments. First of all, 3D-motion correction was conducted to correct the functional EPI scans for motion artifacts. Second, spatial smoothing was performed with a Gaussian filter (FWHM = 5mm). Third, intensity normalization and slice timing correction were performed. Fourth, rigid body transformation was performed to align the functional runs with the high-resolution structural brain image. Finally, a grey matter mask was created to extract the blood-oxygen-level-dependent (BOLD) data from the fMRI scans for further analysis.

Statistical Analysis

Statistical analyses were performed with Matlab and SPSS 22. The normality of the data was checked with the Shapiro-Wilk test using Matlab with customized functions (Öner & Deveci Kocakoç, 2017).

For behavioral data with multiple factors, ANOVA was performed with SPSS 22. If we detected a significant main effect or interaction effect, post-hoc t-tests were performed. Bonferroni correction was used as a multiple correction method in the dissertation. We determined significance after multiple corrections, but uncorrected p-values were reported in the dissertation. Moreover, effect sizes were also reported. Partial eta squared and Cohen's d were reported respectively for ANOVA and post-hoc tests. For brain imaging data, permutation tests were conducted to determine the significance of the dataset.

For model fitting, r-square was used as the parameter to measure the goodness-of-fit.

Aim 1: Whether Feature-Based Plasticity Can Occur Independently and Where in the Brain It Can Occur

Introduction

Previous studies have shown that visual perceptual learning can occur as a result of exposure to a visual feature (Arsenault & Vanduffel, 2019; Bruns & Watanabe, 2019; Galliussi, Grzeczkowski, Gerbino, Herzog, & Bernardis, 2018; Gutnisky et al., 2009; Lorenzino & Caudek, 2015; Pascucci et al., 2015; Protopapas et al., 2017; Rosenthal & Humphreys, 2010; Seitz, Kim, & Watanabe, 2009; Seitz & Watanabe, 2003; Watanabe et al., 2002; Watanabe et al., 2001). We proposed that such learning resulted from changes in the modification in feature representation termed feature-based plasticity.

Several psychophysical studies have attempted to investigate whether feature-based plasticity is independent and where in the brain is associated with the changes of feature-representation as in *Aim 1*. Watanabe et al. (2002) conducted a psychophysical experiment in which subjects performed a center task to detect numbers among letters while a ‘Sekuler display’ was exposed to the subjects as a task-irrelevant stimulus. The Sekuler display consisted of a number of dots moving within a predefined motion range. The Sekuler display not only induced the perception of the dots moving within their local directions, but it also induced the perception of a global motion direction which is the temporal and spatial average of the local motion directions (Williams & Sekuler, 1984). Previous researches have also suggested that the local motion directions were processed in early visual areas V1/V2 while the global motion direction was processed in higher-level visual cortex V3A and beyond (Koyama et al., 2005). After the subjects were asked

to perform the center letter detection task repetitively, the improvement was within the local motion directions. On the other hand, when subjects were asked to perform a task on the discrimination of Sekuler display, the improvement was observed first on the local motion directions but later on the global motion direction. These results suggest that when a visual feature is exposed as task-irrelevant, feature-based plasticity seems to occur independently of task-based plasticity. Moreover, the changes seem to occur in the early visual areas where the features are represented.

However, several factors precluded the conclusion that feature-based plasticity can occur independently in early visual areas. First of all, it is not entirely sure that attention and higher-level task processing has never been associated with the local motion visual features. Although the Sekuler display was exposed as task-irrelevant, it is not guaranteed that subjects did not direct their attention while performing the center detection task. Second, the psychophysical studies did not provide direct evidence for early visual areas' involvement in feature-based plasticity. It is not entirely clear whether other task-related brain regions also contributed to the improvement of feature-based plasticity.

To address Aim 1, we conducted a decode fMRI neurofeedback (DecNef) study with Experiments 1 and 2. DecNef can provide a specific brain activation pattern in a target brain area (Shibata et al., 2019; Shibata, Watanabe, Sasaki, & Kawato, 2011; Watanabe, Sasaki, Shibata, & Kawato, 2017). There was no task involvement or stimulus presentation in the DecNef procedure. DecNef can repetitively induce the brain activation pattern corresponding to a visual feature in a targeted brain region to explore a causal

relationship between brain region changes and behavioral outcomes. In Experiment 1, we induced a brain activation pattern corresponding to the local motion signals in the Sekuler display in the V1/V2. We hypothesize that we will observe changes in local motion directions only without more considerable improvement on the global motion direction, as shown in Figure 3A. This result will suggest that feature-based plasticity can occur independently of task-based plasticity in early visual areas. If more remarkable improvement is induced in the global motion direction as shown in Figures 3B and 3C, this will be inconsistent with our hypothesis. In Experiment 2, we conducted a control experiment to provide further evidence that the results we observed in Experiment 1 were

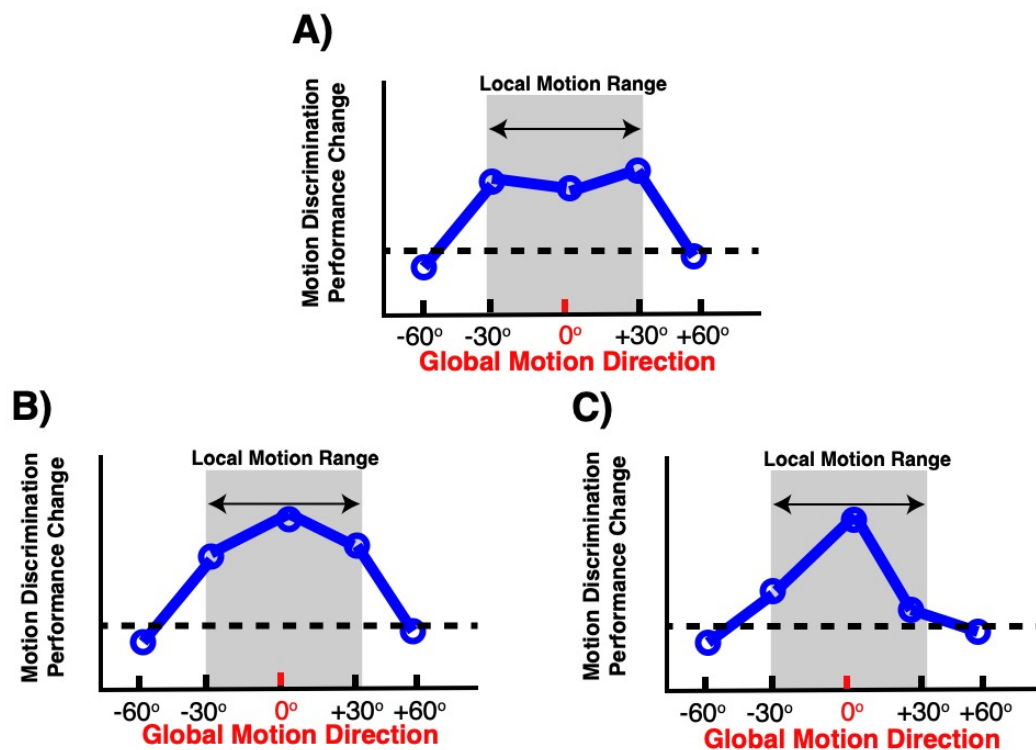


Figure 3 Hypothesis for Experiment 1. A) Only feature-based plasticity is induced with DecNef in V1/V2. B) Both feature-based and task-based plasticity is induced with DecNef. C) Only task-based plasticity is induced with DecNef.

not due to test-retest effects.

Experiment 1

Experiment timeline

Experiment 1 consisted of 4 stages as in Figure 4: the pretest stage, fMRI decoder construction stage, neurofeedback stage, and the posttest stage. The neurofeedback stage consisted of 3 sessions, and the rest stages consisted of only one session. Each session was performed on different days.

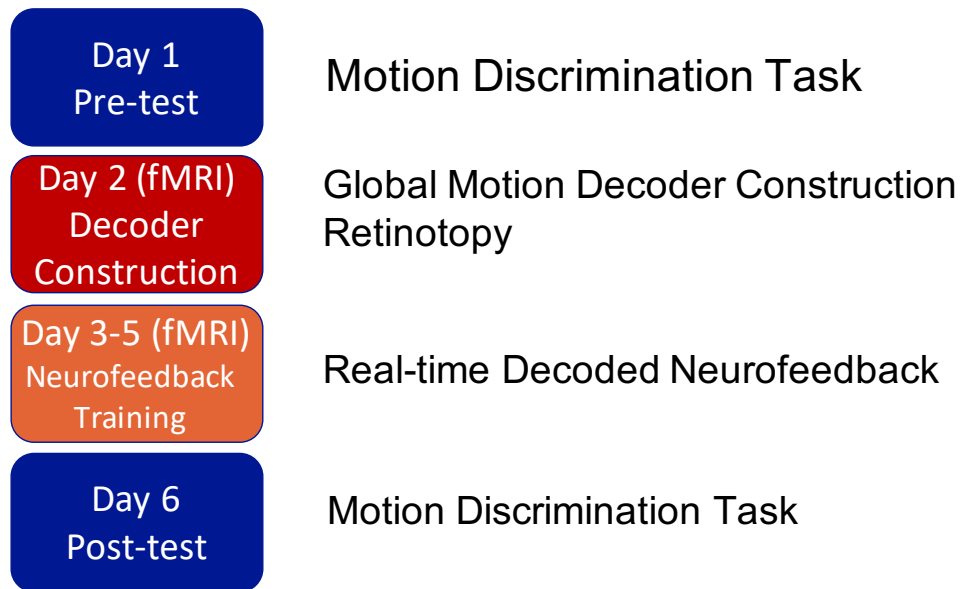


Figure 4. Experiment 1 timeline.

Subjects

Eight subjects participated in Experiment 1.

Stimuli

Two types of motion stimuli were used in the Experiment 1 and 2. The Sekuler display (Williams & Sekuler, 1984) was used during the decoder construction stage, while the coherent motion (Braddick et al., 2001; Salzman, Murasugi, Britten, & Newsome, 1992) was used during the pre and posttest stages.

The Sekuler motion consisted of 100 dots. For each frame, 65 dots moved spatiotemporally locally within a specific range ($-30^\circ - 30^\circ$) of the global motion direction. The signal dots generated the perception of not only the local motions but also the global motions which was the spatiotemporal average of the local motions as in Figure 5A. 35 dots were assigned as noise dots. Noise dots moved randomly. Each frame

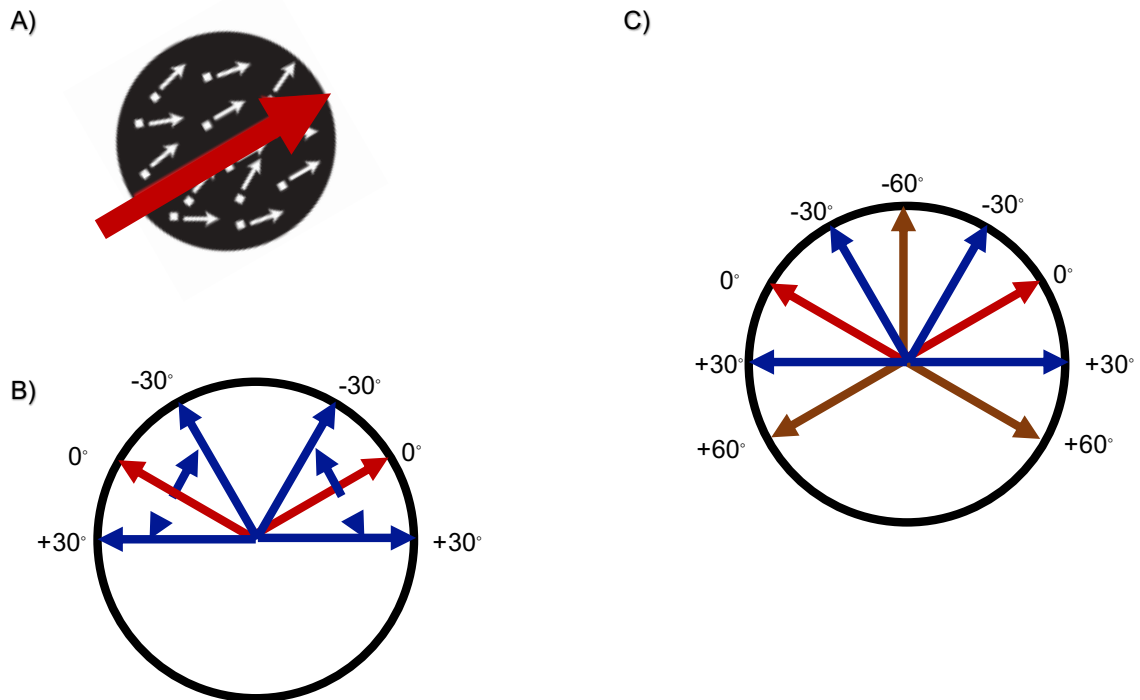


Figure 5 Stimuli in Experiment 1. A) Sekuler display. The global motion is shown as the red arrow, which is the temporal and spatial average of the local motion signals. B) Illustration of the global and local motion directions used in Sekuler motion. The local motion ranges were in blue, while the global motion direction was shown in red. C) Coherent motions that were presented during pre- and posttests consisted of the global motions (red), local motions (blue), and other motion directions (brown).

was presented for 50ms. Two ranges of global motion displays were used. The global motion direction was away from each other to ensure no overlap between the two ranges

of the global motion display as in Figure 5B. One range of the global motion display was selected pseudorandomly as the trained global motion range.

The coherent motion stimuli consisted of 70 dots moving randomly within a 4.5° radius aperture. 10% of the dots were assigned as the signal dots and moved coherently in a predetermined direction at a speed of $7.1^\circ/\text{sec}$. Each from a different set of dots was selected as the signal dots. The rest of the dots (noise dots) were placed randomly within the aperture. Each frame was presented for ~ 16.7 ms. 18 motion directions were tested to cover the range of the global motion direction, the local motion directions, and the motion directions outside of the global and local motion ranges, as shown in Figure 5C.

Pre- and posttest

The sensitivity of each motion direction was measured with 20 trials. The trained and untrained global motion directions and other related motion directions were tested in two different blocks. The order of each of the tested motion directions was pseudorandomized within each block.

In one trial, subjects performed a motion discrimination task. After a 400 ms fixation point, one coherent motion direction was presented for 500 ms. Subjects were then presented with 9 arrows indicating the alternatives and were asked to respond which direction was presented by pressing the keyboard button. D-prime was calculated for each direction as the index for performance. We fitted the tuning curve as a function of the motion directions with a smooth spline with piecewise polynomials. The smoothing parameter was 0.95. The d-prime within the trained and untrained motion ranges were summed as the mean improvement for each subject and then averaged across subjects.

fMRI decoder construction

To acquire the blood-oxygen-level-dependent (BOLD) signal activation patterns corresponding to the two global motion directions, the decoder construction stage was conducted inside MRI with structural brain image acquisition, AutoAlign and functional EPI scans.

The subjects' BOLD activation signals were acquired with EPI runs while they performed a fixation task when two types of global motion stimuli were passively exposed to them pseudorandomly. Each run consisted of 24 trials and lasted for 300 sec. Each trial consisted of a 6 sec stimulus period and 6 sec fixation period. During the stimulus period, the color of the fixation point changed from white to green for 500ms. The fixation point could change color in 12 of the 24 trials. During the fixation period that followed, subjects responded by pressing a button with the index finger if they noticed a color change. Each run started with a 10 sec fixation period and ended with a 2 sec fixation period. At the beginning of the run, the fixation period was inserted for the magnetic field of the scanner to reach equilibrium. There were 10 runs in total.

Retinotopy mapping runs were also acquired with the EPI runs in the same session to delineate each individual subject's visual areas (Engel et al., 1994; Fize et al., 2003; Yotsumoto et al., 2008). The stimuli used during retinotopy mapping were checkboard stimuli that alternated between the vertical and horizontal meridians and upper and lower visual fields. The retinotopic stimuli occupied a smaller radius than the decoder construction stimuli to avoid selecting the stimuli' edges. Each type of checkboard stimuli was presented for 8 sec. There was a 0.01 probability that the color of

the fixation point changed to red on each frame. Subjected responded by pressing a button with their index finger as soon as they noticed the color change.

Decoder construction runs and the retinotopy runs were preprocessed with Freesurfer (Fischl, 2012) as described in the **General Analysis** section, except that no spatial smoothing was performed for the decoder construction runs.

The decode was constructed with a voxel-based intensity analysis. First, V1/V2 were delineated from the retinotopy analysis. Then, the time-courses of BOLD intensities were extracted from the voxels within the V1/V2. The functional data were then shifted by 6 sec, which was assumed to be the hemodynamic delay in this study. The linear trend was removed from the data, and the intensities were z-scored. We created the data sample used to construct the decoder by averaging the intensities from 3 volumes representing the stimulus period. In total, there were 240 data samples with 120 trials for each global motion direction.

The decoder was created by training a sparse logistic regression to the data samples (Miyawaki et al., 2008; Yamashita, Sato, Yoshioka, Tong, & Kamitani, 2008). Sparse logistic regression automatically selected the voxels with the V1/V2 relevant for the separation of the two Sekuler motion types. The regression calculated the weights for the selected V1/V2 voxels as a decoder to separate the representation of the two Sekuler motion types. We conducted leave-one-out cross-validation with 9 runs of the data samples as training samples and the rest run as the test sample. After 10 rounds of cross-validation, we averaged the 10 accuracy scores as the accuracy of the decoder.

Neurofeedback

We applied the decoder acquired for each subject to the neurofeedback stage. The 8th volume from the first decoder construction run was obtained as a template to evaluate the spatial correlations between decoder and neurofeedback sessions in order to avoid motion artifacts in real-time experiments so that the voxels selected during neurofeedback experiments corresponded to the decoders constructed in V1/V2. We performed induction runs during the neurofeedback sessions to induce the trained global motion pattern in V1/V2. Each run lasted for 330 sec, started with a 30 sec fixation period, and consisted of fifteen 20 sec trials. Each trial consisted of a 6 sec induction period, a 6 sec fixation period, a 2 sec feedback period and a 6 sec intertrial interval. During the induction period, a '+' sign was presented at the center of the screen. The subjects were instructed to try to make a later-presented green disc as large as possible. A '-' sign was presented to signal the following fixation period. The fixation period was 6 sec to match the assumed hemodynamic delay. A green disc was presented timely during the feedback period. The green disc's size is proportional to the likelihood of the trained global motion pattern calculated by applying the decoder to the BOLD intensities from the fixation period of the current trial. A '=' sign was presented for the subsequent intertrial interval period. Subjects were instructed to fixate at the center of the display throughout the whole induction run. When no induction was conducted, subjects were instructed to attempt to relax.

The real-time feedback was computed as follows with MATLAB and SPM. 3D motion correction was performed to align each real-time volume to the first volume. A spatial correlation between the current volume and the template image was calculated. If

the correlation is lower than 0.85, the run was then terminated. A new set of structural images was acquired with AutoAlign to ensure the proper selection of voxels with little motion artifact. Then, the BOLD intensities time courses were extracted from the voxels in V1/V2. Later, the time course was detrended and z-scored to the 10 sec – 30sec functional data from the onset of the run. Next, the decoder weights were applied to the averaged time course for three volumes to calculate to the likelihood of the current activation pattern. The disc of the green disc was proportional to the likelihood.

Subjects underwent a mean of 10.63 +/- 1.5 runs during one neurofeedback session. Subjects were encouraged to freely report what strategies they used to finish the task. The strategies summarized in Table 1 were not related to motion.

Table 1. Reported strategies during the neurofeedback stage

	Strategies
Subject 1	Green disk
Subject 2	Visualizing a huge green disk, and it gets larger.
Subject 3	Visualizing green
Subject 4	Emotional argument; Random feelings of life; Imagining some details of a landscape
Subject 5	Happy memories and events; Job and family members; Music and dancing
Subject 6	Visualizing a circle getting larger and small objects
Subject 7	Landscapes images involving green such as ponds and grass; Movie scene from ‘Shining’; Algae; Maintaining fixation and imaging scenes with green elements.

Subject 8	Musical notes and philosophical questions
-----------	---

Offline leak analyses

In order to confirm that the induced patterns in V1/V2 during neurofeedback were confined in the target area, we assessed whether similar activation patterns were also found in other brain regions, namely whether the activity patterns in V1/V2 leaked outside of the targeted area V1/V2. If the activity patterns in other brain areas showed similarity to the induced global motion pattern, this would indicate that the behavioral changes were not driven solely by changes in V1/V2. If, on the other hand, only the activity patterns in V1/V2 were similar to the targeted pattern, this would support our conclusion that activities in V1/V2 drove the behavioral changes.

We used the following ROIs: V1/V2 (the target area during neurofeedback), V3A, the middle temporal area (MT), and the medial superior temporal (MST) area as the potential areas for leakage as these ROIs are closely related to motion processing. We defined V3A, MT and MST using the parcellation published with Freesurfer template brain (Glasser et al., 2016). First, we preprocessed the runs from the neurofeedback stage with Freesurfer, including motion correction, detrending, z-scoring. We created the data samples by averaging the time courses corresponding to the 6 sec induction period. We reconstructed the likelihood of the induced motion pattern in each of the ROIs during neurofeedback with sparse linear regression (Toda, Imamizu, Kawato, & Sato, 2011). We trained the sparse linear regression using data from two sessions and tested the likelihood from the rest of the session. We then transformed the real-time score of the trained motion likelihood with a hyperbolic tangent function since the score we acquired in real-

time was nonlinearly distributed. The reconstruction in each ROI was defined as a Fisher-transformed correlation coefficient between the reconstructed linear regression score and transformed real-time score. The statistical significance was calculated with permutation tests in the following way. First, the reconstructed linear regression score was permuted 1000 times and 1000 correlation coefficients were obtained between the permuted score and the real-time score. Second, we evaluated the reconstructed score in each ROI concerning the permutation distribution. If the reconstructed score was ranked higher than the top % percentile, the score was regarded as significant. Z-score was calculated for between-subject comparisons.

Result

The results section contained the decoder accuracy for the decoder construction stage, the performance for the pre- and posttest stages shown in d-prime as well as the leak analysis.

The mean accuracy of the decoder after cross-validation was significantly higher than 50% chance level [$t(7) = 2.38$, $p = 0.04$, Cohen's $d = 0.842$]. During the neurofeedback stage, we observed an significant increase of the score of the trained Sekuler display pattern with a mean improvement of 5.41 ± 2.11 (SEM), $t(7) = 2.56$, $p=0.038$, Cohen's $d = 0.905$.

Subjects also demonstrated performance improvement on the motion discrimination task, which contained the trained global and local motion ranges. There was no improvement in the untrained global and local motion ranges, as shown in Figure 6. Moreover, there was no significant improvement for the trained global motion

direction [$t(7) = 0.9601$, $p = 0.369$, Cohen's $d = 0.339$] and the untrained global motion direction [$t(7) = 0.046$, $p = 0.965$, Cohen's $d = -0.016$] (0° motion direction in Figure 6)

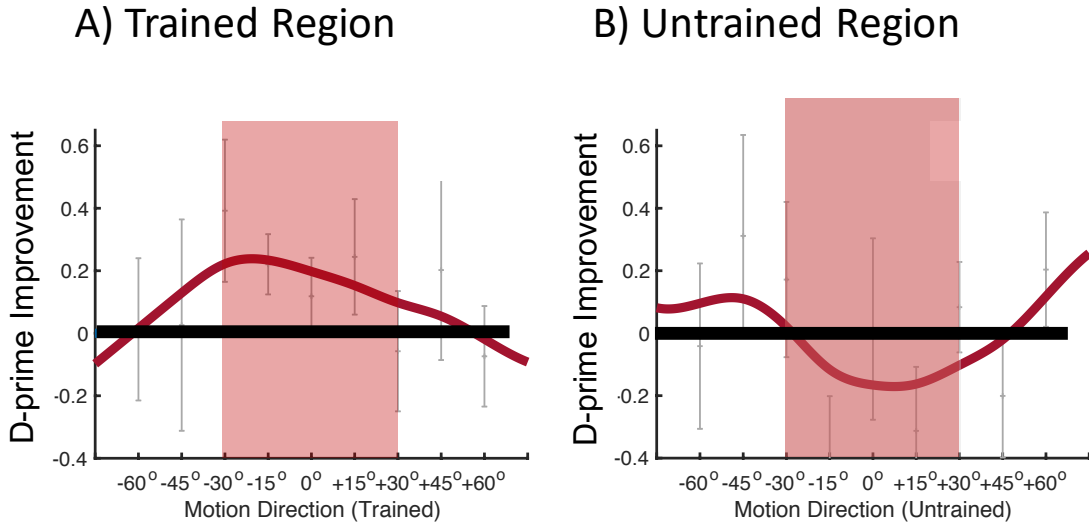


Figure 6 Performance improvement on the motion discrimination task. A) Mean (+/- SEM) improvement in the trained motion range. Improvement was found in the trained local motion ranges. B) Mean (+/- SEM) improvement in the trained motion range. No significant improvement was found. 0° represents the global motion direction. The red line indicates the fitted curve of the tuning function. The shaded area corresponds to the local motion ranges.

We calculated the mean performance improvement in the trained and untrained local motion ranges by summing the improvement in each local motion direction and averaging across subjects. As shown in Figure 7, the improvement in the trained local motion ranges was significantly greater than zero, [$t(7) = 2.57$, $p = 0.037$, Cohen's $d=0.91$]. The improvement in the untrained local motion ranges was not different from zero [$t(7) = -0.866$, $p = 0.415$, Cohen's $d = -0.3062$].

The leak analysis result confirmed that the induced motion pattern was largely confined in the target V1/V2 region. We performed sparse linear regression in V1/V2, V3A, MT, and MST to reconstruct the induced motion pattern's likelihood in each of

ROI. Our results demonstrated that only V1/V2 was able to largely reconstruct the real-time score, reflecting the induced patterns during the real-time neurofeedback stage. The reconstructed score was shown as a Fisher-transformed correlation coefficient in Figure 8. The reconstructed performance was significantly larger than zero for V1/V2 [$z = 8.171, p=0.000$]. There was no other motion-related region that showed a significant reconstruction score greater than zero [MT: $z = 0.498, p = 0.31$; MST: $z = 0.569, p = 0.28$; V3A: $z = -0.421, p = 0.66$]

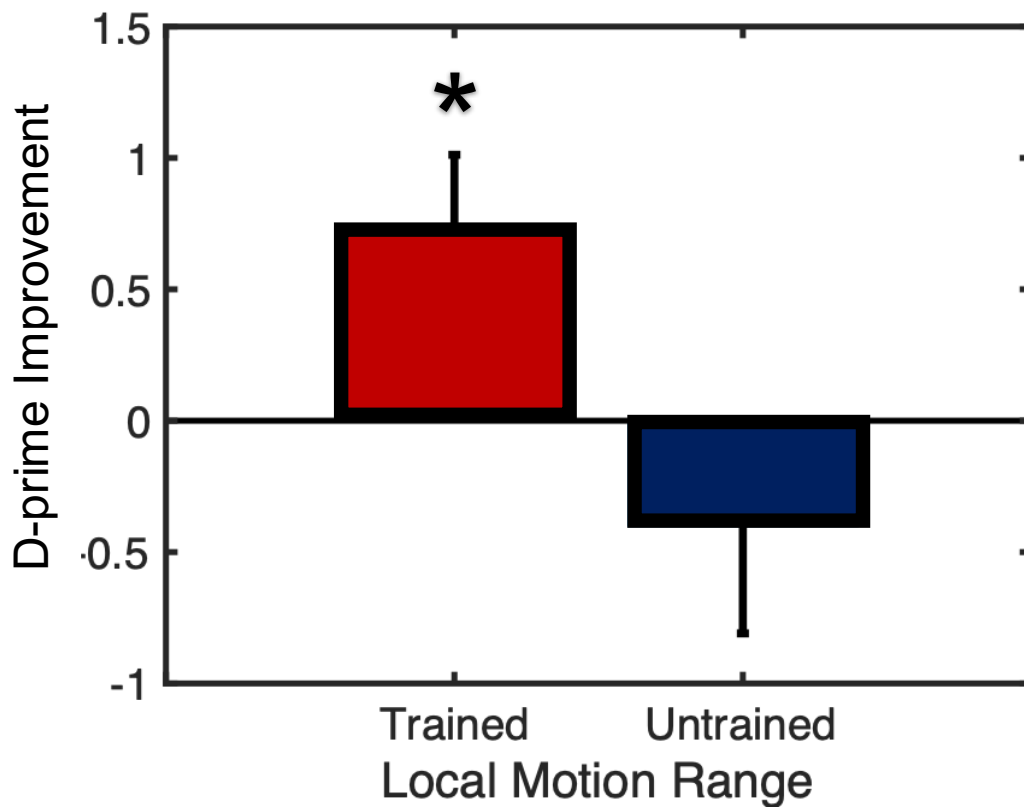


Figure 7 Mean (+/- SEM) improvement for the trained and the untrained local motion ranges.

There was significant improvement only in the trained local motion ranges. * $p < .05$.

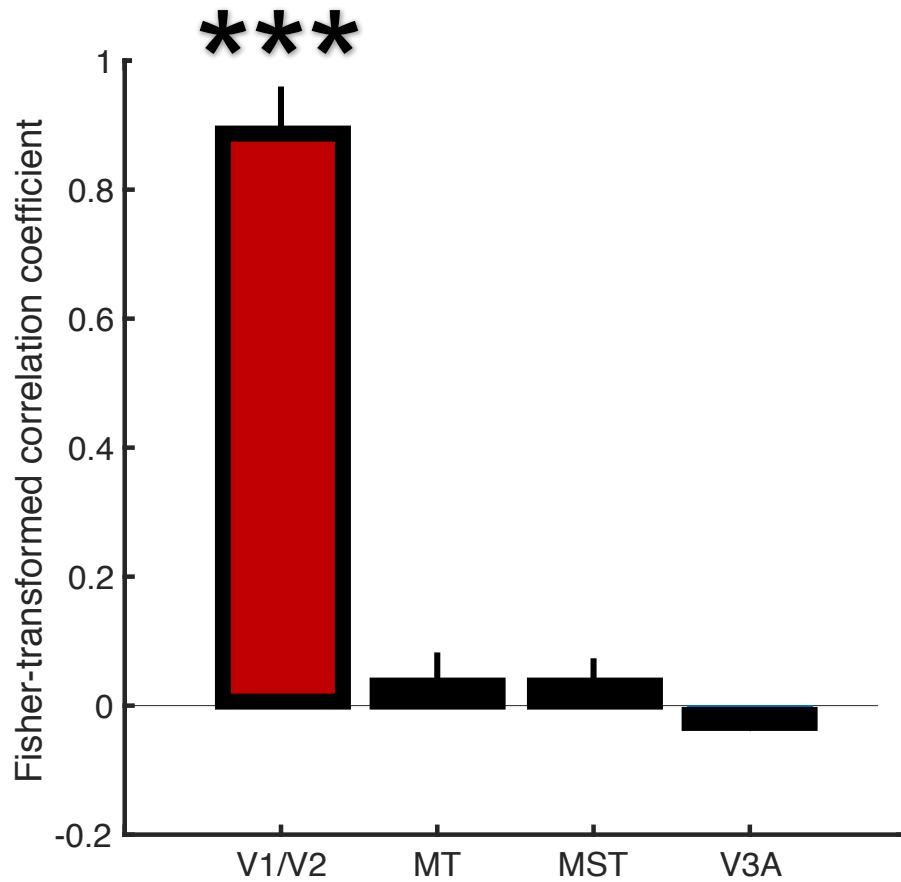


Figure 8. Mean Fisher-transformed correlation coefficient between the induced pattern and the reconstructed score in ROIs. V1/V2 (target ROI) were shown in red, and the other control ROIs were shown in black. Only the activation pattern in V1/V2 (red) can significantly reconstruct the estimated scores of the V1/V2 activation pattern during the neurofeedback stage [$z = 8.171$, $p=0.000$]. *** $p < .001$.

Experiment 2

Experiment 2 was conducted to assess whether the exposure to the global motion stimuli during the decoder construction session has induced the behavioral findings. The

control experiment also aimed to rule out that test-retest effects contributed to the results in Experiment 1.

Experiment timeline

Experiment 2 consisted of 4 stages: pretest stage, decoder exposure stage, rest stage, posttest stage. The pre- and posttest stages were the same as in Experiment 1. The decoder exposure stage consisted of the same stimuli as in the decoder construction stage in Experiment 1. The difference was that the subjects conducted the decoder exposure stage outside of the scanner in a psychophysical room and responded with a keyboard button press. The rest stage was inserted so that the timeline between pre- and posttest stages was similar to Experiment 1.

Subjects

Ten subjects with normal or corrected-to-normal vision participated in Experiment 2.

Results

The subjects' performance for the trained and untrained local direction ranges were calculated as improvement in summed d-prime improvement for each subject and then averaged across 10 subjects. As shown in Figure 9, in contrary to Experiment 1, there was no improvement for clockwise [$t(9) = -1.595$, $p = 0.145$] or counterclockwise local motion ranges [$t(9) = -0.373$, $p = 0.717$]. We further compared whether there was a difference between the two groups using a two-way mixed-design ANOVA with 'direction' as a within-group factor and 'group' as the between-group factor. There was a significant interaction effect [$F(1,16) = 4.631$, $p = 0.047$, partial $\eta^2 = 0.224$]. Moreover, the trained local motion ranges showed significant higher d-prime compared to the

clockwise local motion ranges, [$t(16) = 2.703$, $p = 0.016$, Cohen's $d = 0.676$]. The difference between the Experiment 1 and Experiment 2 demonstrated that the effects were largely related to neurofeedback training rather than confounded by test-retest effects or exposure to the global motion stimuli during the decoder construction stage in Experiment 1.

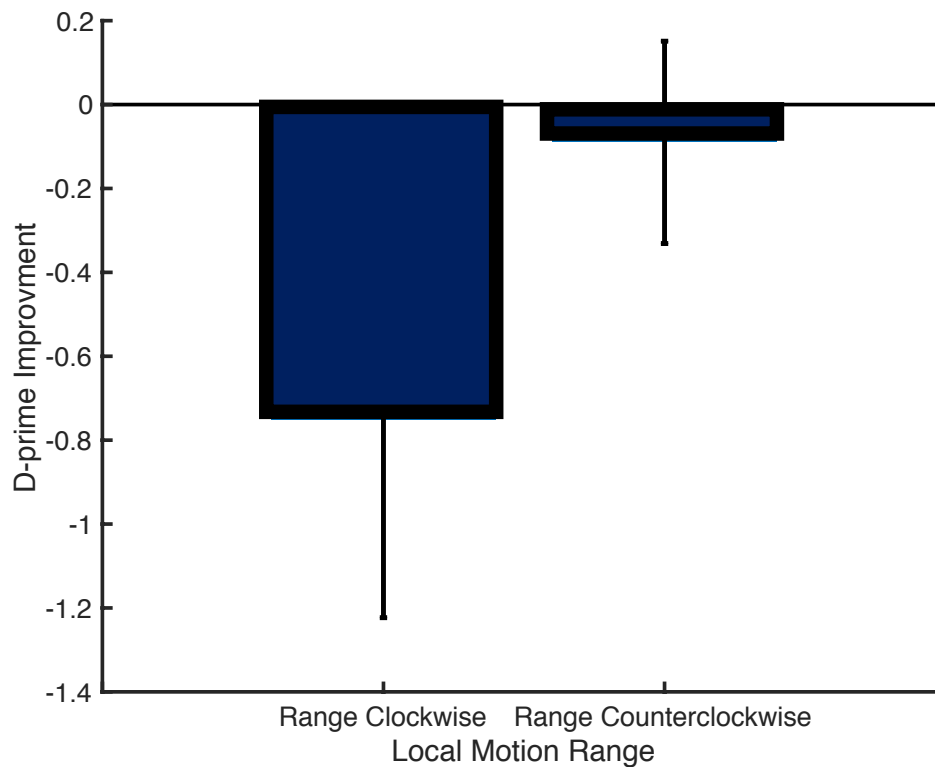


Figure 9. D-prime improvement for local motion ranges in Experiment 2. There was no significant improvement for the clockwise or the counterclockwise local motion ranges.

Discussion and Conclusion

Previous psychophysical results suggest that exposure to a visual feature can induce feature-specific plasticity in early visual areas. However, two problems prevented the ultimate conclusion that feature-based plasticity is independent and feature-based

plasticity of a primitive visual feature originated from early visual areas. First, it is not guaranteed that no attention has been diverted to the exposed visual feature to ensure that feature-based plasticity occurs. Second, psychophysical results can only provide indirect evidence for the brain areas in association with feature-based plasticity. Therefore, in Aim 1, we conducted a series of two experiments, neurofeedback in Experiment 1 and control analysis in Experiment 2, to address the two issues.

In Experiment 1 we trained subjects of the Sekuler display which was known to induce both feature-based and task-based plasticity. The local motions in the Sekuler motion, which corresponded to feature-based plasticity, were repetitively induced in V1/V2 with decoded neurofeedback. The neurofeedback procedure ensured that there was no relevant task that has been performed. Moreover, subjects were never exposed to the stimuli but were only exposed to a brain activation pattern corresponding to the feature in V1/V2. We found that the subjects improved on the local motion directions with no specific improvement to the global motion direction, which corresponded to task-based plasticity. Experiment 1 supported our claim that feature-based plasticity can occur independently irrespective of task-based plasticity. Moreover, we conducted an offline analysis to investigate whether the induced brain activation pattern was only confined to V1/V2. The offline analysis further confirmed that the induced pattern was exclusively restricted in V1/V2. This result suggested that the behavioral improvement was induced by changes in V1/V2, which is consistent with our hypothesis that feature-based plasticity occurred in V1/V2. The results in Experiment 2 further ruled out other confounding factors, such as test-retest effects, etc. Experiment 2 corroborated our findings in Experiment 1.

In conclusion, we found that feature-based plasticity can be developed independently of task-based plasticity. Furthermore, feature-based plasticity is associated with changes in V1/V2. More specifically speaking, the changes in featural representation could explain how feature-based plasticity develops in early visual areas V1/V2.

Aim 2: What Factors Are Involved in the Development of Feature-Based Plasticity

Introduction

In Aim 1, we addressed the controversy about whether feature-based plasticity can occur independently of task-based plasticity. We also investigated the brain regions in association with feature-based plasticity. However, it is unclear what factors are involved in the development of feature-based plasticity.

The reward is one of the most intriguing functions that has been extensively studied related to learning (Rescorla & Wagner, 1972; Schultz, 2002, 2006, 2015, 2016; Schultz, Dayan, & Montague, 1997). The dominant reward model suggests that it is effective on learning through reinforcement and prediction error (Rescorla & Wagner, 1972). Schultz also found that dopamine neurons were activated when rewards occurred at unpredicted time points, signaling prediction error (Schultz, 2002, 2006). Several studies have shown that reward (Frankó, Seitz, & Vogels, 2010; Law & Gold, 2008, 2009; Seitz & Dinse, 2007; Seitz et al., 2009; Xue, Zhou, & Li, 2015) play a critical role in promoting visual perceptual learning. Specifically, Seitz and his colleagues (Seitz et al., 2009) presented a sequence of two orientations in random order, which were made invisible by the continuous flash suppression paradigm (Tsuchiya & Koch, 2004). One orientation was paired with a reward. The other orientation was not paired with reward. All of the orientation stimuli were consistently presented in one eye for each subject. The results showed that performance was enhanced only with the orientation paired with reward, and no transfer was found to the untrained eye. These studies suggest that reward

plays a significant role in VPL, specifically for feature-based plasticity that occurred in early visual areas.

It has also been suggested that arousal level could also be influenced by reward presentation (Aston-Jones & Cohen, 2005; Sara & Bouret, 2012). Salient stimuli can change the arousal level and influence the cortex mediated by locus coeruleus (Sara & Bouret, 2012). Arousal is also part of the attention system's functions, which can increase the rate at which visual stimuli are being sampled (Posner & Petersen). Animal models have suggested that arousal level can enhance the visual cortex's signal-to-noise ratio (Kim, Lokey, & Ling, 2017; McGinley, 2020; Vinck et al., 2015). However, the effects of arousal on feature-based plasticity remain unclear.

We hypothesize that reward affects feature-based plasticity through reinforcement learning rules. Thus, for a visual feature to be learned, the feature needs to be presented before reward so that the feature is predictive of reward.

On the other hand, we hypothesize that arousal affects learning through an enhancement of the signal-to-noise ratio. The effect of arousal can be induced with a salient stimulus regardless of the presentation order of the feature and arousal stimuli. We thus predict that arousal can induce learning of a visual feature when an arousal cue is presented before or after the visual feature.

In Experiment 3 and 4, we investigated the mechanisms of reward and arousal, respectively. To further clarify the effects on the visual cortex, in Experiment 5, we fitted a revised normalization model (Carandini & Heeger, 2011; Reynolds & Heeger, 2009) with the effects of reward and arousal.

Experiment 3

Experiment timeline

The experiment consisted of 4 stages: pretest (1 session), training (12 sessions), posttest (1 session).

Subjects

18 subjects participated in the study. 9 subjects participated in the ‘Reward Before’ group. 9 subjects participated in the ‘Reward After’ group.

Stimuli

Noise masked sinusoidal gratings were presented during test and training sessions. The gratings were orientated 112.5° or 22.5° , with 4° diameter, 10% contrast, and a spatial frequency of 2 cycles/degree. The gratings were presented at the center of an 8° annulus surrounded by a gray background. The 4° to 8° field of the annulus was presented with Gaussian masked random noise. The stimuli were presented at the 0° to 4° of the visual field and were masked by different levels of noise. The noise was generated from a sinusoidal luminance distribution to ensure identical statistical distributions of the luminance for the noise and the gratings. Consequently, there were no texture cues in association with different noise levels. During the pre- and posttest stage, 7 different signal-to-noise levels (SN: 0.03, 0.05, 0.07, 0.1, 0.13, 0.16 and 0.2) were presented pseudorandomly on different trials. During the training stage, a constant SN level of 0.2 for the grating was used.

Pretest and Posttest

Sensitivity tests were performed during pre- and posttest sessions, as shown in Figure 10A. These test sessions were scheduled at least one day apart from the training

sessions. During the test sessions, stimuli were presented to one eye, and a gray screen was presented to the other eye. The testing sessions consisted of 8 blocks, with each block containing 112 trials. Subjects were instructed to align the two screens with the haploscope before starting each testing block. At the beginning of each trial, random noise was presented with a green fixation point for 500ms. The noise was followed by the grating stimuli and a red fixation point for 500ms. The red fixation point will be presented for another 2500ms after the stimuli disappeared. The red fixation point indicated the presence of stimuli and the signal for participants to make responses. Subjects were instructed to decide whether 112.5° or 22.5° grating was presented by pressing the corresponding buttons. 7 SN levels were presented for each of the two orientations in two eyes separately. The 28 conditions were pseudorandomly interleaved with 32 trials for each condition. Subjects were tested for a total of 896 trials in total during the pretest and posttest sessions.

Training

Subjects were trained consecutively for 12 sessions. Each training session was scheduled on different sessions, which were at least 24 hours apart. Subjects were instructed to abstain from eating and drinking for five hours before each training session. Water was provided as a reward to the subjects during the training period. Subjects in the 'Reward Before' group and the 'Reward After' group differed in their timing of receiving the reward. The continuous Flash Suppression (CFS) paradigm (Tsuchiya & Koch, 2004) was used during the training session to render the stimulus invisible to the subjects, as shown in Figure 10C. This procedure reduced the subject's conscious bias of associating grating stimuli with the presence or absence of reward.

We presented an alternating mini-block of 15s CFS stimuli to each eye to ensure contiguous suppression from flash patterns. During the first mini-block, the untrained eye was presented with high contrast flashing noise. The CFS stimuli consisted of a sequence of full-screen textured pattern images presenting at a rate of 10 Hz. The texture pattern consisted of 300 randomly placed, physically overlapping rectangles or ellipses of various sizes with dimensions from 0.5° to 5° . The shapes were of different orientations and saturated colors (0 or 100 cd/m^2). In addition, 50% of the screen was covered with spatially sparse, colored noise. The trained eye was presented with 2Hz noise. Intermittently, a grating stimulus (112.5° or 22.5°) of 0.2 SN was presented to the trained eye for 500 ms. One of the orientations was chosen randomly as the trained orientation. The time interval between the grating stimulus was at least 3000 ms. For the ‘Reward Before’ group, water was delivered 400ms prior to the onset of the trained grating stimulus. For the ‘Reward After’ group, water was presented 400ms subsequent to the presentation of the trained grating stimulus. No reward was paired with the untrained grating stimulus. In both cases, the reward was presented for 500ms, inducing a 100 ms overlap with the stimulus presentation. The overlap was inserted to ensure the processing of reward and maximize the possibility that water reward could be associated with orientation stimulus. After the first 15s mini-block, the trained eye was presented with the CFS stimuli, while the untrained eye was presented with a gray screen. No reward was presented during this 15s mini-block. The 15s mini-blocks alternated for 5 minutes, and subjects were asked to take a 3-minute break after the 5-minute block. These sequences were repeated 6 times per session, yielding a total of 120 trials for the trained and

untrained orientations, respectively. Subjects were requested to adjust the haploscope to align the two screens after each break as shown in Figure 10B.

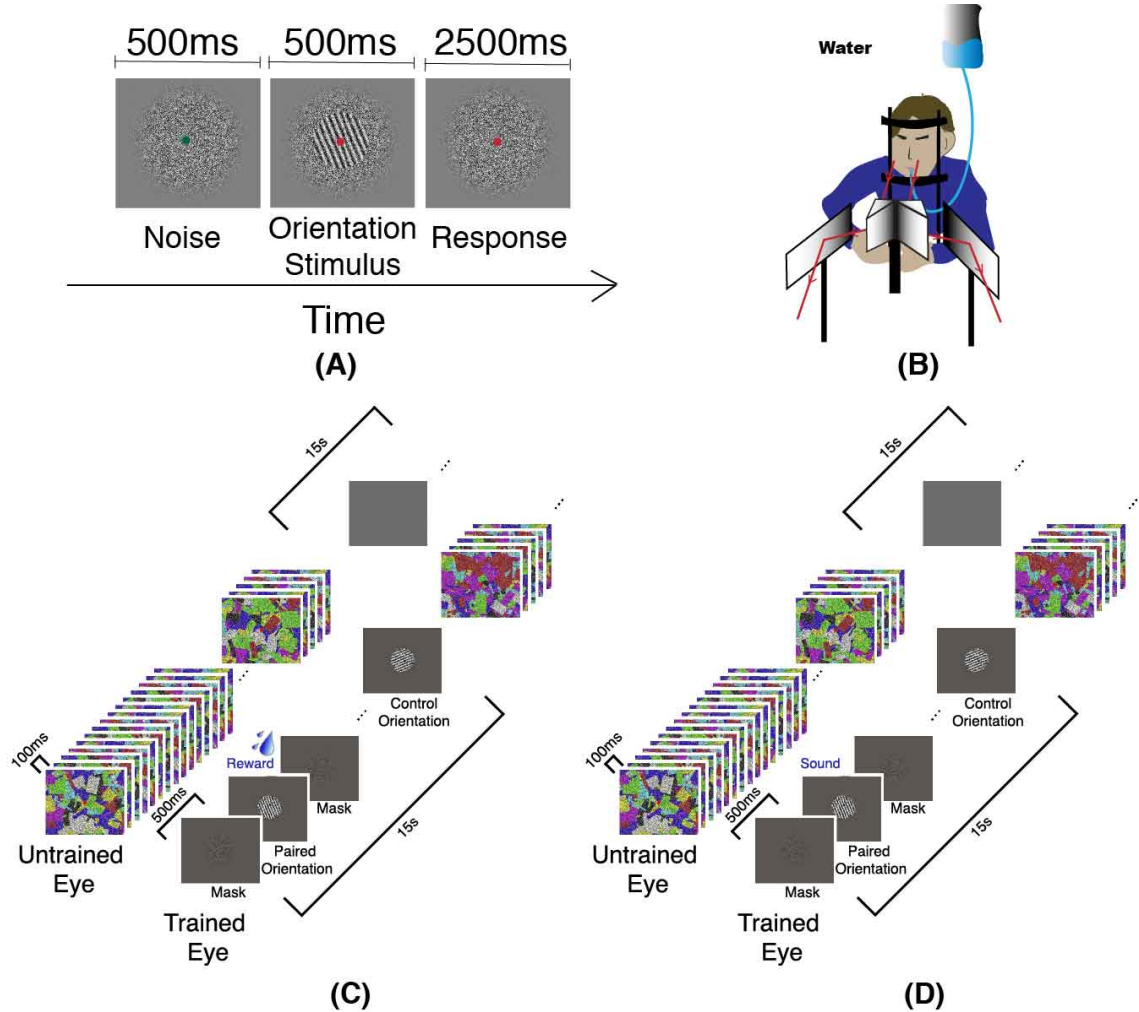


Figure 10. Procedure for Experiment 3 and Experiment 4. A) Orientation detection task in the pre- and posttest stages. Subjects were requested to decide which orientation was presented when the fixation point turned red. B) The illustration of the haploscope and the water delivery device. C) CFS paradigm in the training sessions for Experiment 3. Water reward was paired with the trained orientation in the trained eye. D) CFS paradigm in the training sessions for Experiment 4. Arousal sound was presented in association with the trained orientation. Part of the figure was also shown in the preprint (Z. Wang, Kim, Pedroncelli, Sasaki, & Watanabe, 2019)

Awareness Test

An awareness test was conducted immediately after the posttest. The awareness test was conducted to ensure that the CFS paradigm has successfully rendered the stimuli invisible. Subjects were presented with the same stimuli as in training sessions for one block. During the awareness test, subjects were instructed to decide whether a grating was presented and its orientation by pressing the corresponding buttons. Subjects were also interviewed whether they detected any grating during the awareness test session and the previous training sessions. Subjects were also inquired about whether they were aware of any patterns associated with water delivery timing.

Results

Performance for the orientation detection task was measured as the percentage of correct responses under each S/Ns in the pre- and posttest sessions. The percent correct was shown in Figure 11 for the ‘Reward Before’ and the ‘Reward After’ group in different panels. We performed a three-way mixed-model ANOVA for the Reward group with ‘Orientation and ‘Eye’ as the within-subject factors and the ‘Order’ as the between-subjects factor. The ANOVA showed a marginal significant interaction of Eye x Order interaction, $[F(1, 16) = 4.219, p < .06, \text{partial } \eta^2 = 0.209]$. We also observed a marginal significant interaction of Feature x Order interaction, $[F(1, 16) = 4.286, p < .06, \text{partial } \eta^2 = 0.211]$. we performed post-hoc analysis for each sub-group. For the ‘Reward After’ group, we performed a 2-way repeated-measures ANOVA with ‘Orientation’ and ‘Eye’ as the factors. We found a significant main effect of ‘Eye’, $[F(1,8) = 5.66, p < .05, \text{partial } \eta^2 = 0.41]$ and a marginal significant interaction between the ‘Eye’ and the ‘Orientation’, $[F(1,8) = 4.31, p = .07, \text{partial } \eta^2 = 0.35]$. We performed post-hoc t-tests to each of the

eye and orientation conditions. We found a significant difference between the paired orientation versus the control orientation in the trained eye, [$t(8) = 2.381, p < .05$, Cohen's $d = 0.793$], There is no significant difference between the paired versus the control orientation in the untrained eye. Moreover, the improvement for the trained eye is significantly different from zero with [$t(8) = 4.81, p < .01$, Cohen's $d = 1.60$]. We found no significant ANOVA effects for the 'Reward Before' group, indicating no difference between the conditions. We found no difference between the paired versus the control orientation in either the trained or the untrained eye. For the awareness test, the subjects

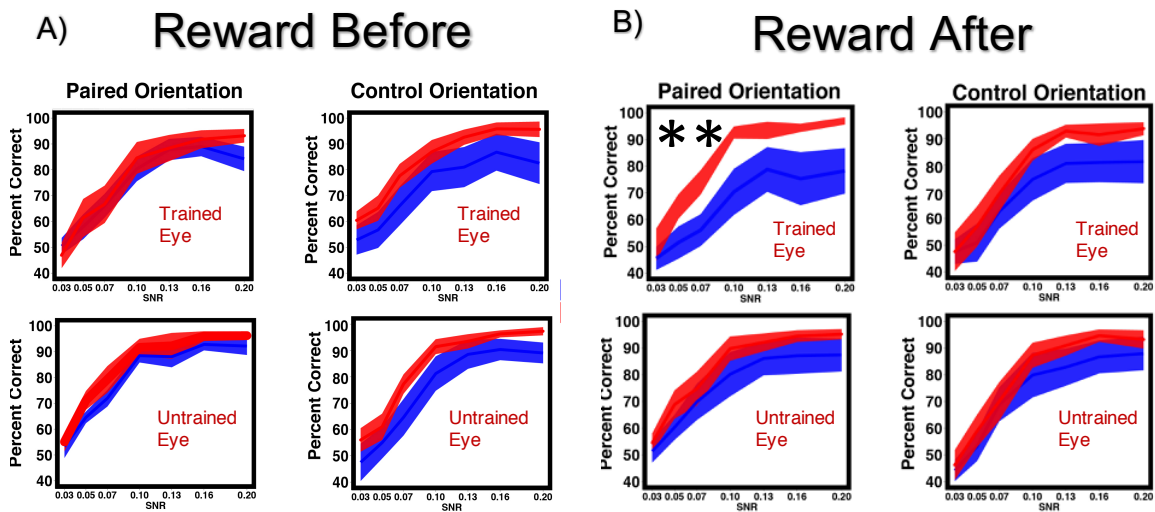


Figure 11. Percent correct change for the 'Reward Before' (A) and the 'Reward After' (B) group.

The percent correct was shown in different panels. The line indicates the mean and the SEM is shown in the ribbon. Blue represents the pretest, and red represents the posttest. Significant improvement was only found for the reward after condition for the paired orientation in the trained eye. * $p < .05$. ** $p < .01$

rarely pressed the button, and the accuracy for correctly recognizing the orientation of the grating was less than 5%. To conclude, there was significant improvement only for the

‘Reward After’ group. Moreover, the improvement was only found for the paired orientation in the trained eye.

Experiment 4

Experiment timeline

Experiment 4 consisted of 3 stages: pretest stage (1 session), training stage (12 sessions), posttest stage (1 session).

Subjects

16 subjects participated in Experiment 4.

Procedure

The experimental procedure for Experiment 4 was primarily similar to Experiment 3. The pretest and posttest stages were the same as in Experiment 3. During the training stage, the visual stimuli and the visual presentation's timing were controlled the same as in Experiment 3. The only difference was that an arousal sound instead of water reward was presented in association with the paired orientation, as shown in Figure 10D. For the ‘Arousal Before’ group, the sound was presented 400 ms before the onset of the paired orientation. For the ‘Arousal After’ group, the sound was presented 500 ms after the onset of the paired orientation. The sound lasted for 500 ms. Subjects conducted the awareness test after the sensitivity test of the posttest session.

Results

Performance for the orientation detection task in Experiment 4 was measured as the percentage of correct responses under each S/Ns in the pre- and posttest sessions. The performance was shown in separate panels in Figure 12. We performed a three-way

mixed-design ANOVA with ‘Orientation’ and ‘Eye’ as the within-subject factor and the ‘Order’ as the between-subject factor. we found a significant effect of Feature, [F(1, 14) = 6.476, $p < .05$, partial $\eta^2 = 0.316$].

We performed post-hoc analyses for the ‘Arousal Before’ and the ‘Arousal After’ group separately. For the ‘Arousal Before’ group, we performed a two-way repeated measures ANOVA with ‘Orientation’ and ‘Eye’ as the factors. We found a significant main effect of ‘Orientation’. We found a significant difference between the paired and the control orientation in the trained eye, [t(7) = 2.675, $p < .05$, Cohen’s $d = 1.00$]. There was also a significant difference between the paired and the control orientation in the untrained eye, [t(7) = 2.408, $p < .05$, Cohen’s $d = 0.91$]. Furthermore, we found a significant improvement in the trained eye for the paired orientation and the control orientation, [t(7) = 3.54, $p < .05$, Cohen’s $d = 1.33$] and [t(7) = 5.10, $p < .05$, Cohen’s $d = 1.92$]. For the ‘Arousal After’ group, the ANOVA did not reveal any between condition differences. However, there was significant improvement in all of the eye and orientation conditions. There was significant improvement for the paired orientation in the trained eye [t(7) = 3.7, $p < .01$, Cohen’s $d = 1.39$], for the control orientation in the trained eye [t(7) = 3.03, $p < .05$, Cohen’s $d = 1.23$], for the paired orientation in the untrained eye [t(7) = 3.48, $p < .01$], Cohen’s $d = 1.31$] and for the control orientation in the untrained eye [t(7) = 3.88, $p < .01$, Cohen’s $d = 1.46$]. Moreover, there was no significant difference between the conditions during the post-hoc analyses. Subjects’ performance during the awareness tests was similar as in Experiment 3.

To conclude, there was a significant improvement when arousal sound was presented before and after the paired orientation stimulus. Moreover, for the arousal

before condition, we found a significant eye transfer. For the arousal after condition, we found a significant eye and orientation transfer.

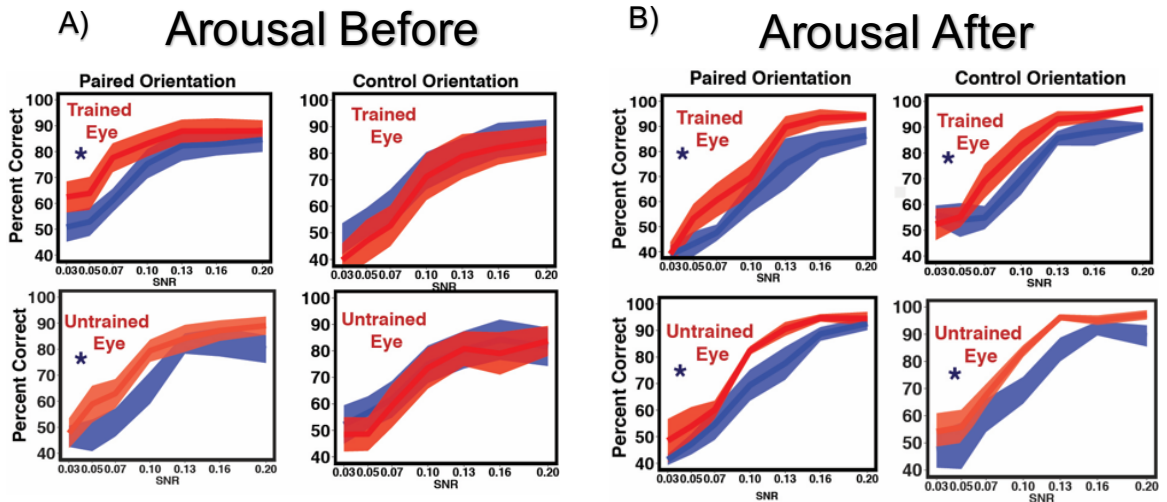


Figure 12. Percent correct change for the 'Arousal Before' (A) and the 'Arousal After' (B) group. The percent correct was shown in different panels. The line indicates the mean, and the SEM is shown in the ribbon. Blue represents the pretest, and red represents the posttest. Significant improvement was found in both groups. * $p < .05$.

Experiment 5: Model Fitting

To individually characterize the effects of reward and arousal in Experiments 3 & 4, we fitted the results with a normalization model that describes the visual system's population response (Carandini & Heeger, 2011; Reynolds & Heeger, 2009). The normalization model was first developed to explain the responses in the primary visual cortex and then proposed to be a universal computation at different sensory systems and other computation levels. The principal motivation was to explain how the primary visual cortex responses are regulated with increasing stimulus intensity. If no regulation were implemented, with the increase of stimulus intensities, the neurons would continue to fire

stronger and ultimately reach their limit. The model proposed that the neurons firing in the primary visual areas were regulated with normalization. The normalization model computes the population responses as the neurons' excitation divided by a normalization factor, which is usually a summation of activities from a pool of neurons. Thus, the population responses from primary visual areas can be described as the excitation normalized by pooled responses as in Equation 1. The excitation $E(x, \theta)^n$ is the summed activity in the neurons' population with different orientation and spatial location preferences and is driven by the stimulus. The excitation was acquired by convoluting an orientation and a spatial location filter to the stimulus. The normalization factor consists of a constant σ and the pooling of responses over spatial locations and orientations for a broader range of neurons $N(x, \theta)^n$. The pooling is computed as the suppressive field $s(x, \theta)$ convoluted with the excitation driven by stimulus (Equation 2). The convolution is computed assuming independence of orientation and spatial location pooling. The exponent n represents the rectification to the shape of firing for primary visual cortex neurons which is usually 2.

$$R(x, \theta) = \frac{E(x, \theta)^n}{\sigma^n + N(x, \theta)^n} \quad (1)$$

$$N(x, \theta) = s(x, \theta) * E(x, \theta) \quad (2)$$

To illustrate the effects of reward and arousal, we added the reward field $R(x, \theta)$ and the arousal field $A(x, \theta)$ as an additional factor to the stimulus drive (Equation 3). We assumed independent effects of arousal and reward. Based on the psychophysical findings, we regarded the effects of arousal to be more excitatory and the

reward effects to be more suppressive. The model's normalization factor was computed as the suppressive field convoluted with the stimulus responses integrating the reward and arousal effects.

$$R(x, \theta) = \frac{\frac{A(x, \theta)}{R(x, \theta)} E(x, \theta)^n}{\sigma^n + N(x, \theta)^n} \quad (3)$$

$$N(x, \theta) = s(x, \theta) * \frac{A(x, \theta)}{R(x, \theta)} E(x, \theta) \quad (4)$$

A schematic illustration of the model is shown in Figure 13. The stimulus was represented as the excitation as stimulus drive. The arousal field and reward field were

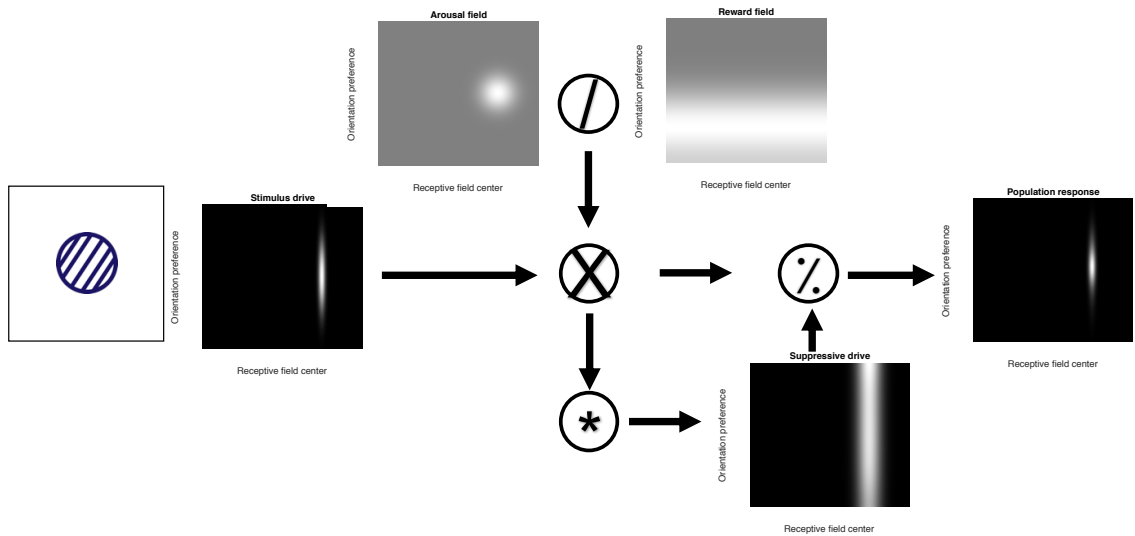
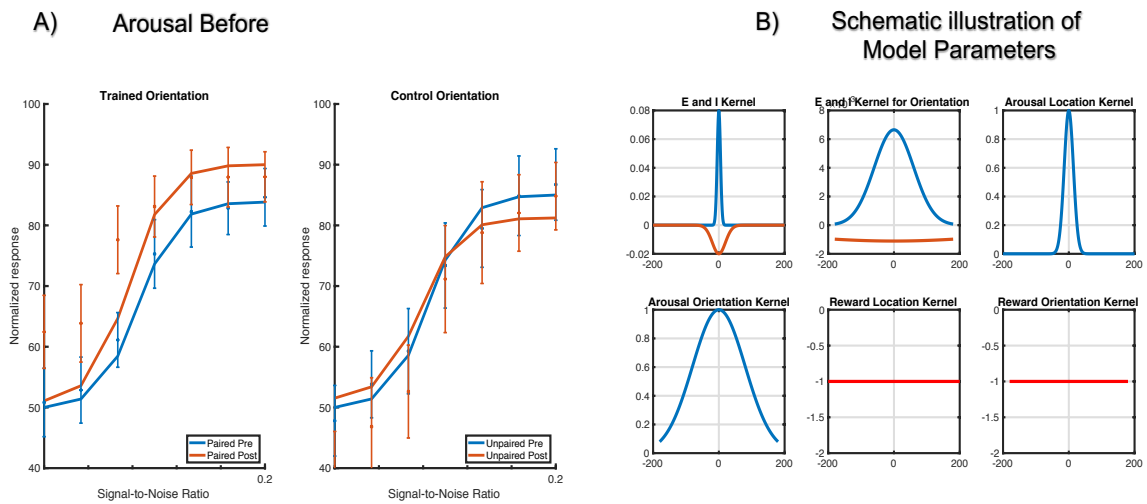


Figure 13. A normalization model of reward and arousal. The model consisted of stimulus drive, arousal, and reward field. The three effects were multiplied to construct the overall excitation, which was the nominator of the model. The nominator was convoluted with the inhibitory field to generate the model's suppressive drive, which was the denominator of the model. The population response was acquired by the overall excitation divided (normalized) by the suppressive drive. added to the stimulus drive to generate the numerator's overall signal. A suppressive field was convoluted with the excitation to generate the suppressive drive for the denominator.

The normalization response was the excitation drive divided by the suppressive drive. Additionally, the population response was linearly transformed to be consistent with the range of the psychophysical responses.

Results

We fitted the model to the behavioral measurements in Experiment 3 and Experiment 4. We only fitted the results with trained and control orientation since the model did not account for eye specificity. The pretest condition was fitted with a model



$$R^2 = 0.82$$

Figure 14. Model fitting for the 'Arousal Before' condition. The goodness-of-fit was 0.82. A) Comparison between model and psychophysical data. The model was shown in lines, and the psychophysical data was shown in dots with error bars representing the SEM. B) Schematic illustration of model parameters. 0 indicated the trained orientation and spatial location.

in which there was no arousal or reward modulation. The model was fitted with only the stimulus drive normalized by the suppressive field. The posttest was modeled for

different experimental conditions with the arousal and reward field. For the ‘Arousal Before’ condition, we observed behavioral improvement in the paired orientation but no transfer to the control orientation. The posttest for trained orientation and the control

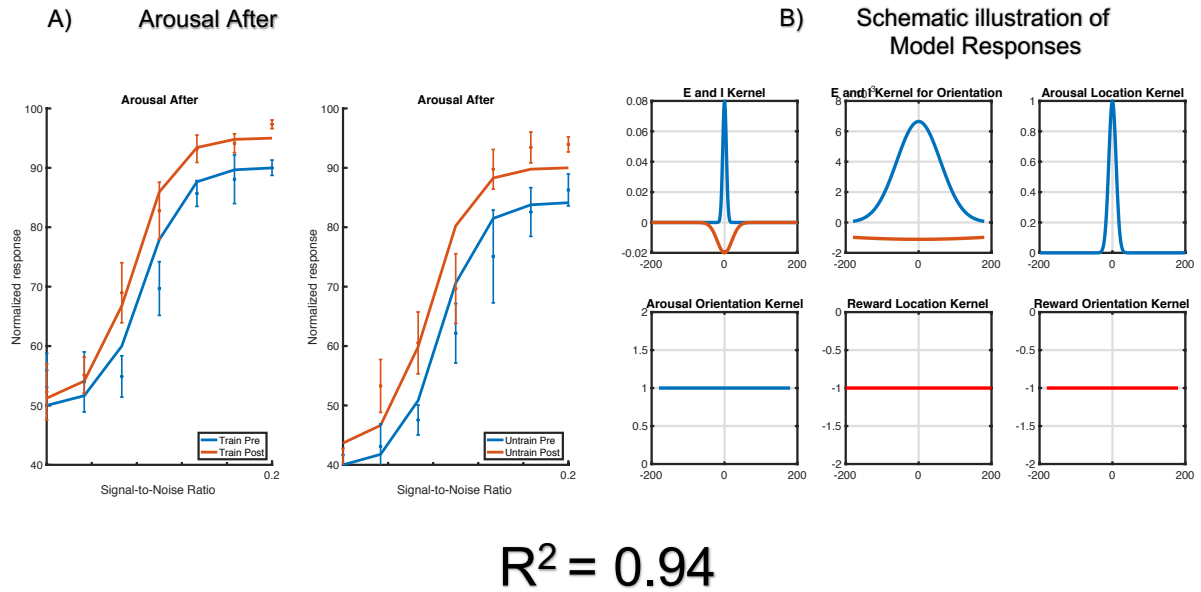


Figure 15. Model fitting for the ‘Arousal After’ condition. The goodness-of-fit was 0.94. A) Comparison between model and psychophysical data. The model was shown in lines and the psychophysical data was shown in dots with error bars representing the SEM. B) Schematic illustration of model parameters. 0 indicated the trained orientation and spatial location.

orientation was extracted from the population response tuned to different orientations.

The best-fitted model was shown in Figure 14 below. The goodness-of-fit was measured with r^2 , which equals 0.82 for this model. The first two figures demonstrated the kernels for stimulus drive and the kernels for the suppressive field. The arousal effects were modeled by a pointed location kernel and a wider orientation kernel. 0 on the x-axis demonstrated the trained orientation. The ‘Arousal Before’ condition was modeled with a

specific enhancement to location and a broader enhancement to the orientation surrounding the trained orientation. The ‘Arousal After’ condition was shown in Figure 15. Unlike the ‘Arousal Before’ condition, there was no effect of arousal orientation kernel. On the other hand, there was a sharp response to the arousal location kernel. The goodness-of-fit was measured with r^2 , which equals 0.94 for this model.

The reward conditions incorporated both the effects of arousal and reward. For the ‘Reward Before’ condition, we found that the best-fitted model incorporated both the

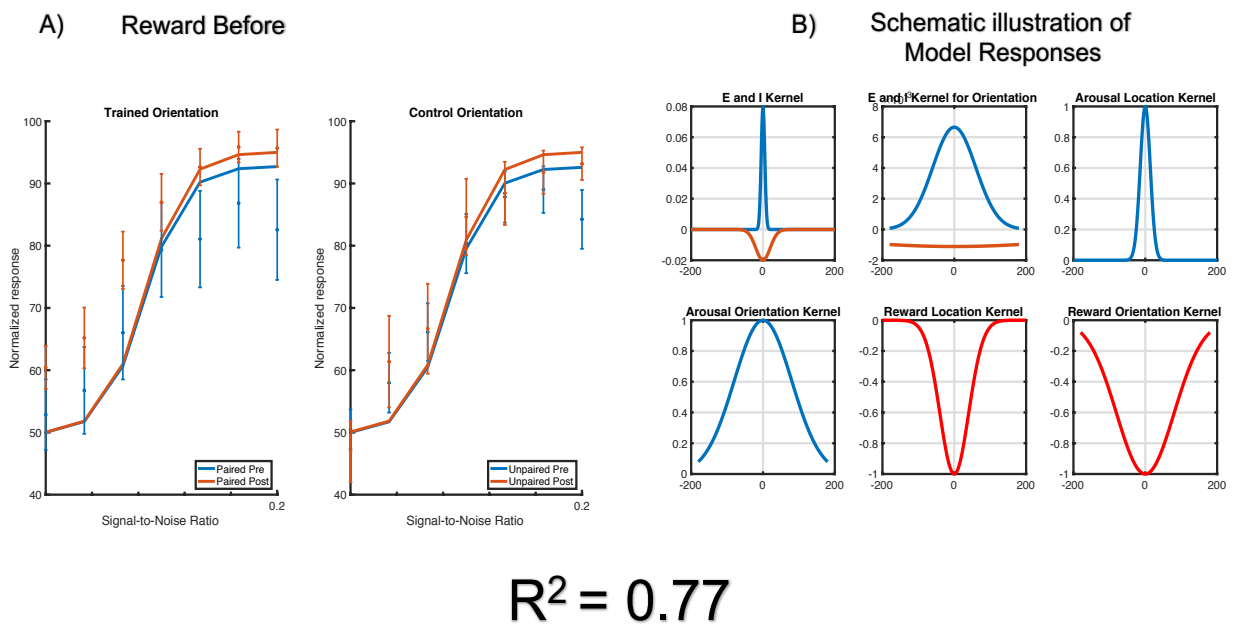


Figure 16. Model fitting for the ‘Reward Before’ condition. The goodness-of-fit was 0.77. A) Comparison between model and psychophysical data. The model was shown in lines and the psychophysical data was shown in dots with error bars representing the SEM. B) Schematic illustration of model parameters. 0 indicated the trained orientation and spatial location.

reward and arousal as in Figure 16. The effects of arousal were modeled the same as in Figure 14. In addition, the reward kernel was to both the location and the orientation

kernel to the paired orientation and spatial location. The reward kernels were modeled as negative since the arousal field was divided by the original model's reward field. The 'Reward After' condition was also modeled incorporating both the orientation and the location kernels, as shown in Figure 17. The goodness-of-fit was measured with r^2 , which equals to 0.77 for this model.

The arousal effects were modeled as in the 'Arousal after' condition. Moreover, there were no effects of reward to the location. There were inhibitory effects to the orientations surrounding the trained orientation. The goodness-of-fit was measured with r^2 , which equals to 0.81 for this model.

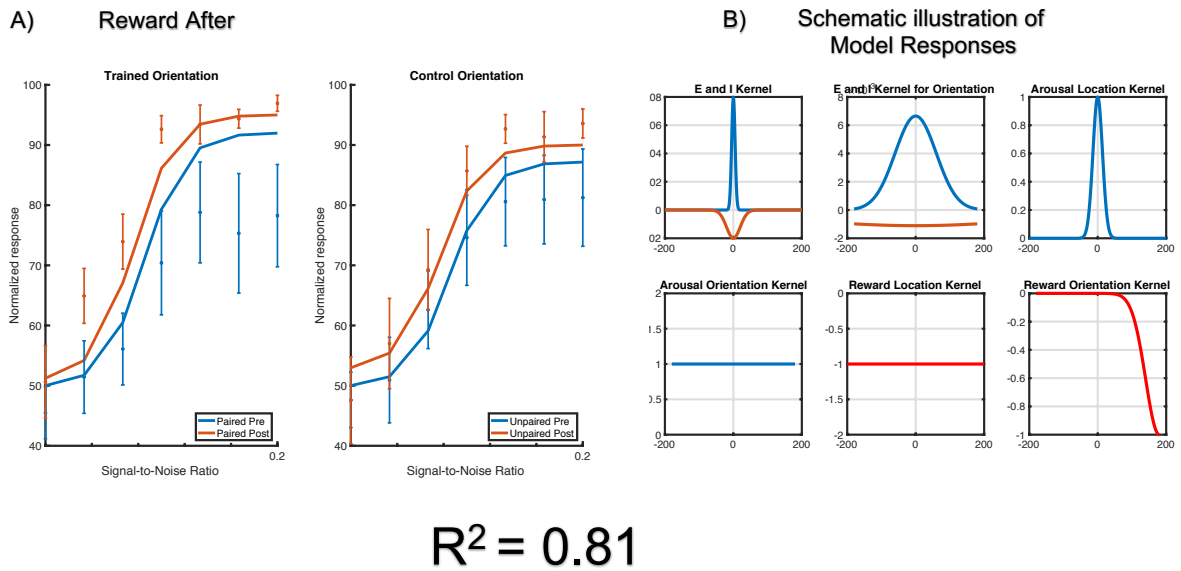


Figure 17. Model fitting for the ‘Reward After’ condition. The goodness-of-fit was 0.81. A) Comparison between model and psychophysical data. The model was shown in lines, and the psychophysical data was shown in dots with error bars representing the SEM. B) Schematic illustration of model parameters. 0 indicated the trained orientation and spatial location.

Discussion and Conclusion

Aim 2 intends to illustrate the effects of reward and arousal on feature-based plasticity. In Experiment 3, we found that reward only induces learning when the reward is presented after the visual stimulus. Moreover, the learning in association with reward is specific to the trained orientation and the trained eye. In Experiment 4, we found that arousal induces learning differently. Arousal both presented before and after the stimulus can induce learning of the trained orientation. Moreover, arousal presented before the

visual stimulus also induces a transfer to the untrained eye. Arousal presented after the visual stimulus also induces transfer to the untrained orientation and the untrained eye.

The psychophysical results indicate that arousal has an excitatory effect, whereas reward has an inhibitory effect on the visual cortex. To quantify the effects of reward and arousal on feature-based learning, we applied the normalization model to the current psychophysical datasets. The parameters from fitting the model indicated that arousal presented before the stimulus has a broader excitatory field compared to arousal cues presented after the stimulus. Furthermore, reward cues presented before the stimulus can be best modeled by a larger inhibitory field, and the reward cues presented after the stimulus can be best modeled by a restrictive field to the untrained orientations. In order to clarify the excitatory or inhibitory effects of reward and arousal, future experiments need to be conducted to directly measure the inhibitory or excitatory activation of neurotransmitters in the brain (Shibata et al., 2017).

Interestingly, the psychophysical results implied that feature learning driven by arousal might be in accordance with the physiological findings in the locus-coeruleus norepinephrine (LC-NE) system. The LC-NE system's phasic activities will fluctuate with different levels of arousal in an inverted U-shaped curve (Aston-Jones & Cohen, 2005). The activities are lower when the arousal level is either high or low. The phasic activities within the LC-NE system reach the maximum with mid-level arousal. Moreover, the phasic activities are associated with regulating the decision-making areas where fewer specificities are observed. Moreover, pre-cues are associated with a higher level of arousal compared to post-cues. Therefore, we speculate that the post-stimulus sound might have a better effect in inducing generalization due to an appropriate arousal

level. On the other hand, the pre-stimulus sound might have a weaker effect in generalization since the arousal level might be beyond the ideal peak. Furthermore, the result cannot be simply explained by attention since attention would have predicted the opposite result as in the current findings. As pre-cues would induce higher focused attention than post-cues, we would expect the pre-stimulus sound to have a larger generalization, which is the opposite of what we found. which is the opposite to what we found. Therefore, our findings indicate that the effects were not driven by focused attention.

One may also argue that the cues in the arousal condition may be useful as a reward. However, we argue here that this scenario is implausible. First of all, the sound was also presented in the reward condition, yet different results were acquired. Second, in the reward group, the subjects abstained from drinking and eating for five hours before coming to the experiment. However, in the arousal group, no fasting was required from the subjects to lower the possibility that any value will be associated with the arousal cues. Finally, subjects were interviewed whether they had knowledge of where the sound was coming from or if they associated the sound with any visual stimuli. None of the subjects reported associating the sound with the stimuli.

One potential argument that may undermine the conclusion in Aim 2 was the lack of direct measurement of arousal level indicated by the pupils' diameter (Bijleveld, Custers, & Aarts, 2009; Leuchs, Schneider, Czisch, & Spoormaker, 2017; Vinck et al., 2015). In the current Experiment 3 and 4, measuring pupils' dilation was restricted due to the use of haploscopes. In future studies, a control group can be recruited without the haploscope to measure arousal and reward cues' effects on the arousal levels. The control

group can supplement the current argument about feature-based plasticity in association with change in arousal levels.

To conclude, in Aim 2, we illustrated potential excitatory effects of arousal on feature-based plasticity and the inhibitory effects of reward on feature-based plasticity.

Aim 3: Higher Level Visual Features: Plasticity and Application

Introduction

Aim 1 and Aim 2 focused on the feature-based learning of a primitive visual feature, such as the orientation of a grating or the directions of the moving dots. However, two significant challenges remain unaddressed by the previous results. First of all, the mechanisms of feature-based plasticity with natural and socially relevant images remain elusive. The perception of natural and socially relevant images is an essential component of everyday life. For instance, face detection is a critical component of social context. Detecting low spatial frequency face components has been associated with identity and rapid emotional detection (Duchaine & Yovel, 2015; Vuilleumier, Armony, Driver, & Dolan, 2003). Natural and socially relevant images usually contain richer visual details across a wide range of visual features. Therefore, given the limited number of studies, it is unclear how feature-based learning can be developed for natural and socially relevant images. Despite recent studies on clinical images (Frank et al., 2020) and a previous study on face view discrimination (Bi, Chen, Zhou, He, & Fang, 2014), there is a limited number of studies that trained subjects to detect complex and socially relevant stimuli like faces. It is also unclear whether feature-based learning was developed for natural images with these two studies. Second, visual perceptual learning has been proposed to be a promising tool for patients with visual deficits from early visual areas, such as amblyopia (Levi, 2012; Polat, 2009; Polat et al., 2004; Polat et al.,

2009; Rosa et al., 2013) and macular degeneration (Astle et al., 2015; Maniglia et al., 2016; Maniglia et al., 2020; Plank et al., 2014). However, visual perceptual learning mechanisms among patients whose visual deficits originated from higher-order visual areas remain unknown.

In Aim 3, we hypothesize that feature-based plasticity for natural images occurs in the networks representing the visual components. Just as for primitive visual features, the feature-based changes occur in early visual areas; the changes for natural images will occur in representing the complex visual features. Moreover, we hypothesize that the changes in complex feature representation will occur in patients as well.

Body dysmorphic disorder (BDD) is a psychiatric disorder defined as having distressing thoughts and preoccupation with slight defects in appearances and particular faces. Body dysmorphic disorder affects 1% to 2% of the population (Beilharz, Castle, Grace, & Rossell, 2017; Li, Arienzo, & Feusner, 2013; Phillips, 2009). Previous studies have suggested that BDD patients have deficits in holistic visual processing, and specifically an imbalance between holistic and featural processing of faces (Beilharz et al., 2017; Feusner, Moller, et al., 2010; Kerwin, Hovav, Helleman, & Feusner, 2014; Li et al., 2013). When performing a low spatial frequency face-matching task, BDD patients showed higher left hemisphere blood-oxygen-level-depend (BOLD) activities in the lateral prefrontal and temporal regions in the dorsal face processing pathway of the brain (Feusner, Moody, et al., 2010; Feusner, Townsend, Bystritsky, & Bookheimer, 2007). Recent studies have highlighted the temporal-parietal junction (TPJ)'s role in the face and social processing. TPJ and, in particular, left TPJ plays a vital role in representing others' beliefs (Samson, Apperly, Chiavarino, & Humphreys, 2004; Saxe &

Kanwisher, 2003). The abnormal dorsal activities shown in the previous BDD studies at least partially overlapped with the TPJ (Arienzo et al., 2013; Feusner, Moody, et al., 2010; Feusner et al., 2007). Moreover, BDD patients showed hypoactivity in the left occipital cortex when performing low spatial frequency tasks than normal controls (Feusner, Moody, et al., 2010), suggesting an imbalance between hemispheric activities. Furthermore, BDD patients demonstrated abnormal functional connectivity globally in the bilateral occipital regions and between FFA and occipital regions (Arienzo et al., 2013; Moody et al., 2015).

On the other hand, holistic visual processing in healthy control subjects is associated with low spatial frequency faces and is processed mainly in the fusiform face area (FFA) in the ventral pathway (Duchaine & Yovel, 2015; Goffaux et al., 2011; Grill-Spector, Knouf, & Kanwisher, 2004; Haxby & Gobbini, 2011; Nancy Kanwisher, McDermott, & Chun, 1997; N. Kanwisher & Yovel, 2006; Richler & Gauthier, 2014; Rossion et al., 2000; Rotshtein, Vuilleumier, Winston, Driver, & Dolan, 2007; Yovel, 2016).

To conclude, the processing of low spatial frequency faces dissociates between the BDD patients and the healthy control subjects. While BDD patients likely represent low spatial frequency components with both the dorsal and the ventral face processing pathways as well as more left hemisphere activities, the healthy control subjects represent low spatial face components with more right hemisphere activities (Duchaine & Yovel, 2015; A. Harris & Aguirre, 2008, 2010; Haxby & Gobbini, 2011; Rossion et al., 2000; Schiltz & Rossion, 2006) majorly in the ventral pathway. Therefore, if our hypothesis is correct and feature-based learning for complex visual features develops in the

representation change, we predict that the changes in BDD patients will occur in both the ventral and dorsal processing pathways. On the other hand, the changes for healthy control subjects will occur only in the ventral processing pathway. Moreover, we predict that no changes will occur in other brain regions that lack the representation of low spatial frequency face components.

Experiment 6

Subjects

A total of 9 subjects with BDD (22 - 52 years, mean 34.9 +/- SD 11.34) and 10 healthy control subjects of a similar age range (20 – 60 years, mean 27.8 +/- SD 11.81) participated in the study. BDD patients consisted of 8 females and one male. Healthy control subjects consisted of 5 females and 5 males. The larger portion of females in the BDD group might be related to a more significant portion of female patients willing to seek medical care than male patients on the population level (Phillipou & Castle, 2015). The healthy control subjects were recruited through Brown University, and the BDD patients were recruited through Rhode Island Hospital. All subjects have given written consents approved by Brown University and Rhode Island Hospital's institutional review board. Healthy control subjects were all pre-screened of psychiatry disorders and psychoactive medications. BDD patients were diagnosed with respect to the DSM-V criteria. All subjects have a normal or corrected-to-normal vision.

Experiment timeline

The study consisted of 4 stages as shown in Figure 18C: sensitivity measurement stage (1 session), pretest stage (1 session), training stage (6 sessions), and posttest stage (1 session). The pre- and posttest stages were conducted in the MRI scanner. The pre-

and posttest stages contained structural image acquisition, task measurement, functional connectivity measurement, and regions-of-interest measurement. The sensitivity measurement and training stages were conducted in a dimly lighted psychophysical testing room outside the MRI scanner. Each session was scheduled at least one day apart.

Stimuli

For the sensitivity measurement stage and task measurement during the pre- and posttest stages, a set of face images with neutral facial expressions and house images were used, as shown in Figure 18A. We created four stimulus categories with spatial

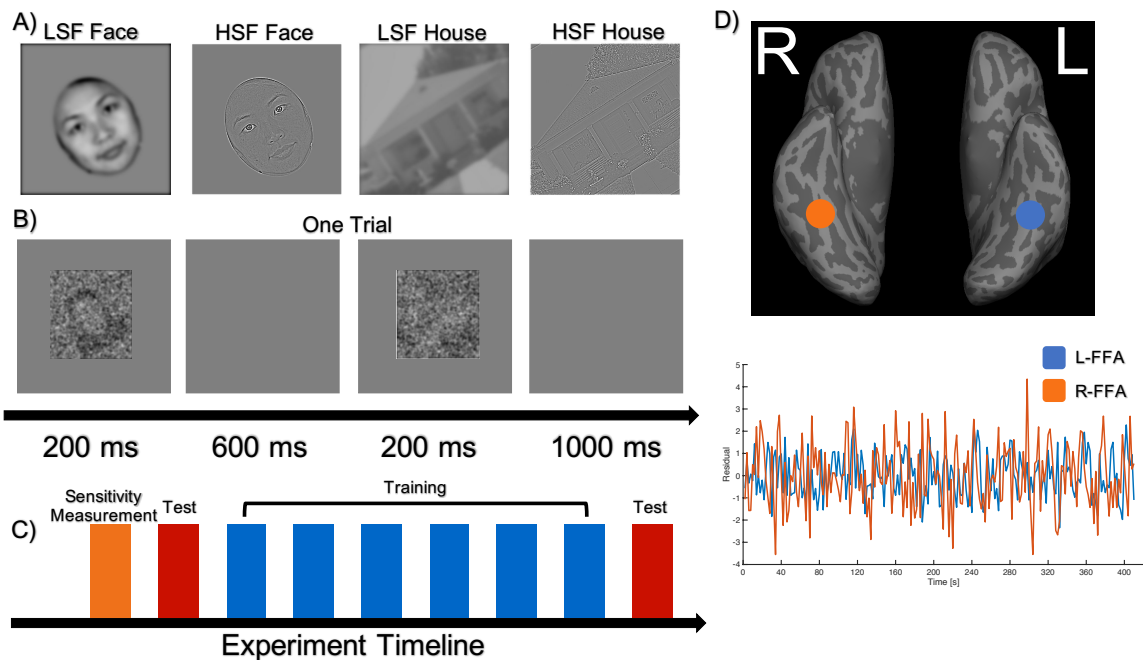


Figure 18. Methods for Experiment 6. A) Illustration of four types of visual stimuli used during sensitivity measurement, pre- and posttest stages. The stimuli include low spatial frequency (LSF) and high spatial frequency (HSF) face and low and high spatial frequency house. B) One trial in the 2IFC task. C) Experiment timeline. The red box indicates sessions that were conducted in the MRI. D) Example for functional connectivity. The figure shows the time course of residuals used in functional connectivity from the left and right FFA.

frequency filtering. The low spatial frequency (LSF) face and house categories contained frequency components that were less than 10 cycles/degree. The high spatial frequency (HSF) face and house categories contained frequency components that were greater than 15 cycles/degree. Each category contained four unique face/house images. During the training stage, only the LSF face category was used. 12 unique face images were used during the training stage. The face images used during training were different from the sensitivity measurement and testing stages to ensure that the training effects were not the result of learning a specific face image but a result of learning to detect LSF components of faces. The images were in greyscale, and the contrast of the images was matched. The face and house images were tilted 45° from the upright position to make the task challenging for the subjects. The stimuli were created by replacing certain portions of the pixels of the images with random Gaussian noise. The background was grey except for a center white bull's eye on a grey disc with a radius of 0.75°.

During ROI measurement, standard images for localizing fusiform face area (FFA) and parahippocampal place area (PPA) were used. These images contained upright faces, phase scrambled faces, upright houses, and phase scrambled houses.

Sensitivity measurement

The purpose of the sensitivity measurement is to obtain each subject's threshold for detecting the face and house stimuli in different spatial frequencies. Subjects performed a two-interval-forced-choice (2IFC) task as shown in Figure 18B. Each of the image categories of each of the spatial frequency components was tested in different blocks. Each trial contained two 200ms stimulus intervals with a 600ms fixation period in between. The trial ended with a 1000ms interval in which the subjects made a response.

One of the stimulus intervals contained a stimulus overlaid with Gaussian noise, and the other stimulus interval contained only noise. Subjects responded whether the first or the second interval contained the stimulus by pressing “1” or “2” on a keypad. The signal-to-noise (S/N) level was controlled with a 3-down-1-up procedure equivalent to an ~84% accuracy rate. The initial S/N ratio was 25%. The step size of the staircase was 0.05 log units. After 10 staircase reversals, the testing block ended. The S/N ratio threshold was calculated as the geometric mean of the last six reversals.

Pretest and Posttest

The pre- and posttest stages consisted of structural image acquisition, task measurement, functional connectivity measurement, ROI measurement. First, during the structural image acquisition, a T1-weighted sequence was conducted to acquire a high-resolution structural brain image of each subject. Second, for the task measurement, subjects performed the 2IFC tasks on the face and house stimuli of each of the low and high spatial frequency components. At the same time, their blood-oxygen-level-dependent (BOLD) activity was measured with fMRI. In total, there were four stimulus categories. The task measurement consisted of 6 fMRI runs in a blocked design. Each run lasted 150 secs and consisted of twelve 12-sec mini blocks. Each mini block consisted of 6 trials and measured only one image category. Each trial lasted for 2 sec and consisted of two 200ms stimulus intervals with a 600ms interval in between and a 1000ms fixation interval. The S/N ratio level for each of the stimulus categories was set to the threshold that had been measured during the sensitivity measurement stage. Additionally, each run started with a 4 sec fixation period and a 2 sec fixation period. The fixation period was added at the beginning of each run for the scanner's magnetic field to reach equilibrium.

Throughout the run, subjects were instructed to maintain their fixation at the white bull's eye in display center. Third, ROI measurement was conducted with two fMRI runs of a 1-back task in which the participant responded whether the current face or house stimulus matched the previous image. Each run lasted 200 sec. Fourth, functional connectivity was acquired with a 410 sec fMRI run while subjects were instructed to maintain their fixation at the center of the display.

Training

The training stage was conducted in a dimly lighted psychophysical room over 6 sessions. Subjects performed the 2IFC task of a face image with only low spatial frequency components. Each session consisted of 10 blocks. Each block was controlled with the 3-down-1-up staircase procedure. The initial S/N ratio was 25%. The step size of the staircase was 0.05 log units. After 10 staircase reversals, the training block ended. The S/N ratio threshold of each block was calculated as the geometric mean of the last six reversals. Subjects performed around 500 trials for each session.

fMRI data processing

Preprocessing

The fMRI runs from the pre- and posttest sessions were preprocessed with the Freesurfer (Fischl, 2012) software. First, each run underwent 3D motion correction. The runs from each measurement section were corrected to the first volume from the first run of that measurement section as a template. For example, the task measurement runs were corrected to the first volume of the first task measurement run, and the ROI measurement runs were corrected to the first volume of the first ROI measurement run, etc. Second, spatial smoothing was performed with a Gaussian filter (FWHM = 5mm). Third, a gray

matter mask was created. Fourth, intensity normalization and slice timing correction were performed. Finally, rigid body transformation was performed to align each template run to the high-resolution structural image.

ROI definition

ROI related to face processing was defined functionally and structurally on each subject's left and right hemisphere individually. A general linear model (GLM) model assuming a gamma-shaped hemodynamic response function (HRF) with a delay of 2.25 sec and a dispersion of 1.25 sec was fitted to the BOLD data from ROI measurement. The model was also fitted with nuisance regressors, including the motion correction regressors, the polynomial drift regressors and temporal whitening. The fusiform face area (FFA) and the occipital face area (OFA) were defined with a contrast of face vs. scrambled face. The parahippocampal place area (PPA) was defined with a contrast of house vs. scrambled house. These ROIs were defined to include all of the voxels that passed the threshold ($p < .001$, uncorrected). Left and right temporal-parietal junctions (TPJ) were defined anatomically as all of the voxels with a 5mm radius range of the average of the published Talairach coordinates ($x = 54, y = -47, z = 28$ and $x = -54, y = -47, z = 28$). The early visual areas were defined anatomically with the Freesurfer parcellation.

Task measurement

The general linear model (GLM) model with the same gamma-shaped HRF function was fitted to the BOLD data from task measurement. The model was also fitted with the same nuisance regressors. The model included four conditions from the task measurement: low spatial frequency face, high spatial frequency face, low spatial

frequency house, and high spatial frequency house. Beta coefficients for each condition were extracted from the general linear model.

Functional connectivity

To investigate the brain connectivity changes in association with training, we analyzed the functional connectivity using the resting states BOLD data. First, nuisance regressors were created for the functional connectivity data. There are four nuisance regressors: the cerebrospinal fluid, the white matter, motion correction parameters, slice time correction with a fifth-order polynomial. Second, GLM models with the nuisance regressors were fitted to the BOLD data from each of the following ROIs as the target ROI: left FFA and left TPJ. The residual of each fitted GLM model was extracted. Third, we selected the right FFA, the left and right OFA as the pair ROIs. We fitted the BOLD data from the pair ROIs with the GLM models and the residual terms were extracted. The residual terms from the left FFA and right FFA from one subject was shown in Figure 18D. Fourth, functional connectivity was measured as a fisher-transformed correlation coefficient between the error term of each pair of the target ROIs and the pair ROIs.

Results

We trained the body dysmorphic disorder (BDD) patients and healthy control subjects on a 2IFC detection task of low frequency face component over 6 sessions. We compared their performances on detecting faces and houses of different spatial frequencies during pre- and posttests. We found that both the BDD group and the healthy control group improved detecting face images of low spatial frequency components, as shown in Figure 19. The improvement was calculated as the (posttest accuracy – pretest accuracy) / pretest accuracy × 100%. We performed a mixed-design ANOVA with

‘Group’ as the between-subject factor and ‘Condition’ as the within-subject factor. There was a significant main effect of ‘Condition’ [$F(3, 51) = 4.547, p = 0.007, \text{partial } \eta^2 = 0.211$]. We further conducted post-hoc t-tests for each condition in the BDD and healthy control group separately. We found that there was a significant improvement for the low spatial frequency face for the BDD group [$t(8) = 3.892, p = 0.005, \text{Cohen's } d = 1.29$] after multiple correction. There was a significant improvement in the healthy control group [$t(9) = 2.775, p = 0.02, \text{Cohen's } d = 0.91$] before multiple correction. There was no significant improvement in the other conditions for the BDD and the healthy control group. There was no difference between the BDD group and the healthy control group [$t(17) = 1.829, p=0.085$].

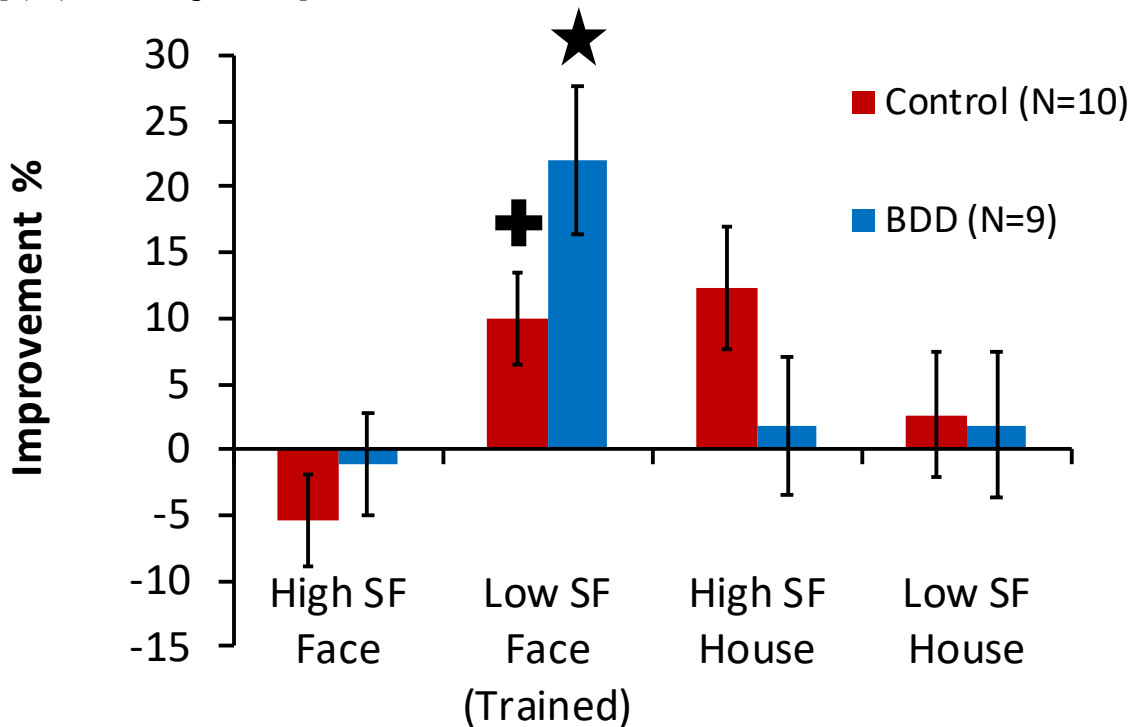


Figure 19. Performance improvement for the BDD (N = 9) and the control group (N=10). Both groups showed significant improvement only for the low spatial frequency face, which was the trained condition. + $p < .05$ before multiple corrections. * $p < .05$ after multiple corrections.

We further measured the BOLD activities change in association with the learning of face images of low spatial frequency components. Previous studies have suggested that BDD patients showed higher activation in the left temporal and parietal region (left TPJ) in association with the processing of low spatial frequency faces compared with healthy control subjects. Moreover, low spatial frequency faces in healthy control subjects have largely been associated with ventral pathway activities. Thus, we hypothesized that training of low frequency face components would affect the processing in the left temporal parietal junction (TPJ) only in the BDD group. We measured the beta weights in association with face images of low and high spatial frequency components. We calculated a beta index as the beta weights of low spatial frequency components minus the high spatial frequency components' beta weights. The beta index measured during pre- and posttests for BDD and healthy control groups when they performed the face tasks were shown in Figure 20A. We performed a mixed-design ANOVA with a between-subject factor as the 'Group' and a within-subject factor as the 'Test'. We found a significant interaction effect between the two factors [$F(1,17) = 4.576, p=0.047$, partial $\eta^2 = 0.212$]. We performed a post-hoc t-test for each condition in each subject group separately. For the BDD group, the beta index measured during posttest decreased significantly compared to the beta index measured during pretest, [$t(8) = 3.07, p=0.015$, Cohen's $d = 0.7$]. There was no significant change for the healthy control group, [$t(9) = 0.561, p = 0.589$]. The results indicated that after training on detecting face images of low spatial frequency components, the BOLD activation in left TPJ decreased for low spatial frequency faces as compared to high spatial frequency faces only in the BDD group. Moreover, we measured the beta index for house perception as the difference between

low spatial frequency houses and high spatial frequency houses. As shown in Figure 20B, there were no significant changes in the left TPJ in association with house perception.

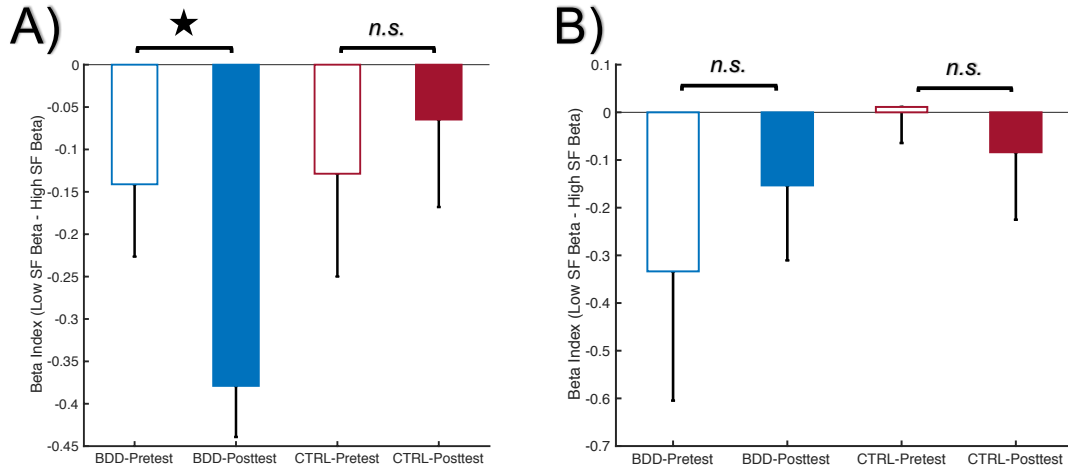


Figure 20. BOLD activation in the left temporal parietal junction (TPJ) for the face (A) and house (B) stimuli. A) There was a significant decrease in the BOLD activation in the left TPJ of the BDD subjects after VPL training. There was no change for the healthy control group. B) There was no change in association with the house stimuli. * $p < .05$.

Second, we measured the BOLD activity in the left and right FFA, which was part of the ventral face processing pathway. Previous studies have suggested that low spatial frequency components are processed dominantly in the right FFA, and BDD patients have deficits in low spatial frequency components. Moreover, BDD patients demonstrated higher left hemisphere activities in the left hemisphere. We, therefore, hypothesized that training BDD patients on low spatial frequency faces would induce changes in the left and right FFA. We measured the dominance of right hemisphere activity of FFA as a right lateralization index. The right lateralization index was calculated as $\text{rightFFA}[\text{beta}(\text{low spatial frequency}) - \text{beta}(\text{high spatial frequency})] - \text{leftFFA}[\text{beta}(\text{low spatial frequency}) - \text{beta}(\text{high spatial frequency})]$. The right

lateralization index for the BDD group and healthy control group during pre- and posttest measurements was shown in Figure 21A. We performed a two-way mixed-design ANOVA with 'Group' as the between-subject factor and 'Test' as the within-subject factor. There was a significant interaction effect of Group x Test [$F(1, 17) = 15.936, p = 0.001, \text{partial } \eta^2 = 0.484$]. Post-hoc t-tests showed that there was a significant increase in right lateralization index for the BDD group [$t(8) = 3.009, p = 0.017, \text{Cohen's } d = 1.003$] and there was a significant decrease in right lateralization index for the healthy control group [$t(9) = 2.6137, p = 0.028, \text{Cohen's } d = 0.827$]. The results indicated that the BDD group increased their BOLD activities in the right FFA compared to the left FFA when processing faces of low spatial frequency components. Moreover, the healthy control group decreased their BOLD activities in the right FFA compared to the left FFA when processing faces of low frequency components. Furthermore, there was a significant Pearson correlation between the changes in right lateralization index and behavioral improvement in BDD patients, as shown in Figure 23 [$r = 0.780, p = 0.013$]. We further tested whether the effect could also be observed in association with house images' perception, as shown in Figure 21B. We performed the two-way mixed-design ANOVA and no significant interaction effect [$F(1,17) = 2.042, p = 0.17$], no significant main effect of Test [$F(1,17) = 1.434, p = 0.248$] or Group [$F(1,17) = 0.550, p = 0.468$].

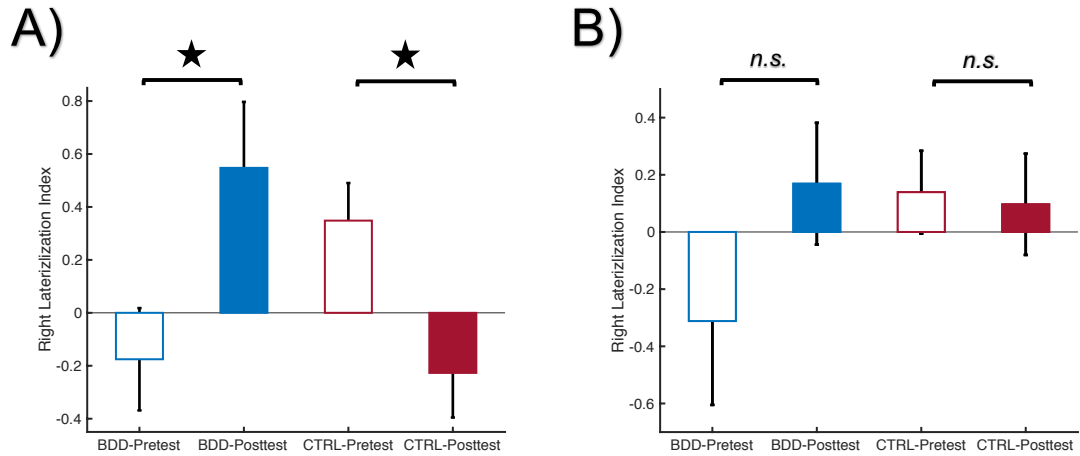


Figure 21. BOLD lateralization index in the FFAs for the face (A) and the house (B) stimuli. A) The right lateralization index for the face stimuli. There was a significant increase in the right lateralization index for the BDD group. There was a significant decrease in the right lateralization index for the healthy control subjects. B) There was no significant change in association with the house stimuli.

Third, we measured the BOLD activity change in early visual areas to test whether the changes in association with low spatial frequency faces were specific to the face processing networks. We did not observe significant BOLD activity change in the early visual areas (V1) in association with the training of low spatial frequency face images in the BDD and the healthy control group, all p s $>.05$ (Figure 22).

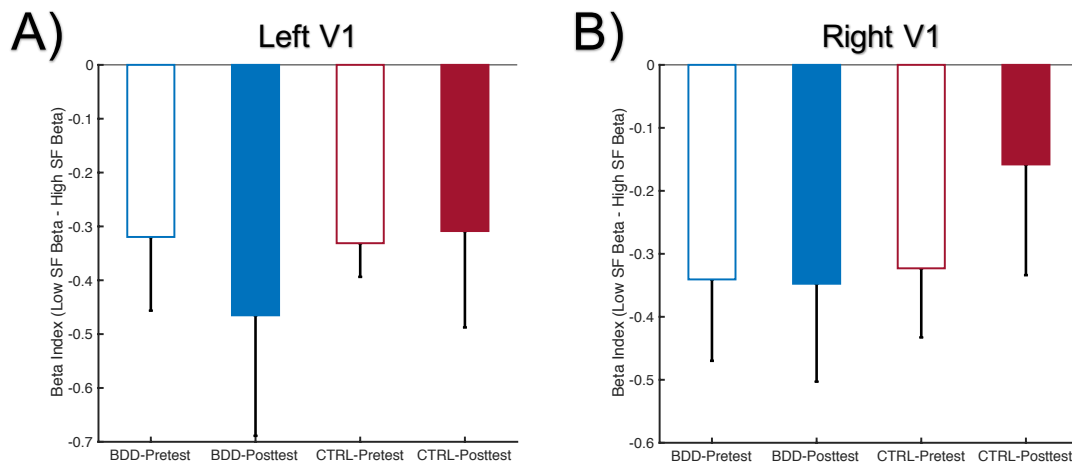


Figure 22. BOLD activation change in the left V1 (A) and the right V1 (B). There was no BOLD activation change in the left or the right V1 for the BDD or the healthy control subjects.

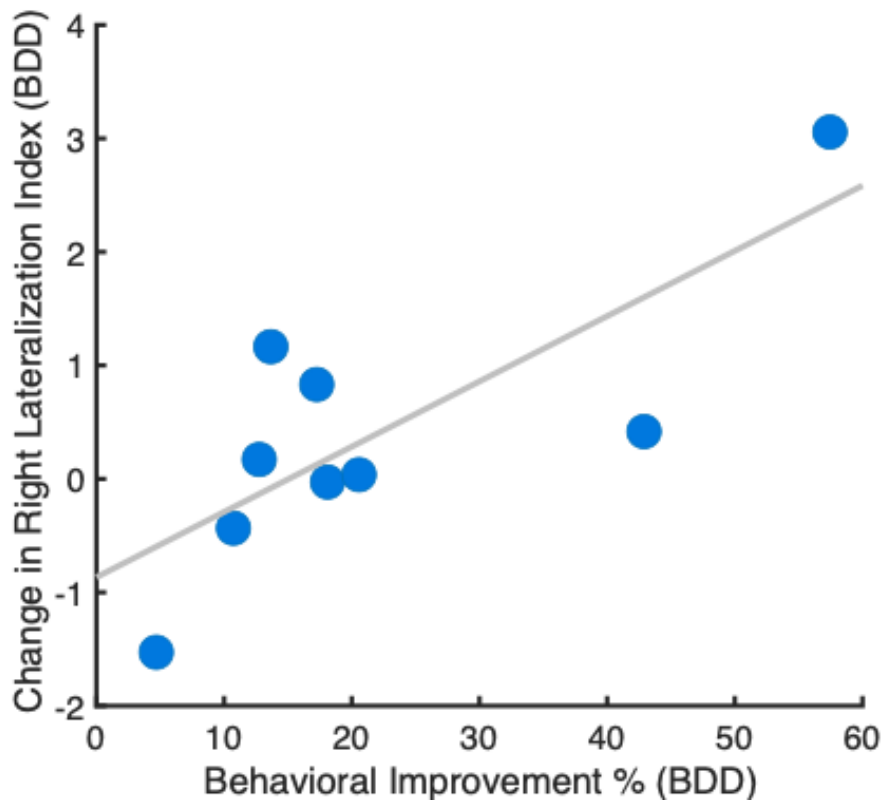


Figure 23. Correlation between the BOLD change in right lateralization index and the performance improvement in the BDD group.

We measured functional connectivity changes between the dorsal and ventral pathways and the connectivity changes within the ventral pathways using fisher-transformed correlation coefficients. First, we measured the functional connectivity using the TPJ as the target ROI. We found a significant functional connectivity change between the TPJ and the left OFA, as shown in Figure 24A. A two-way mixed-design ANOVA with ‘Group’ as the between-subject factor and ‘Test’ as the within-subject factor showed a significant effect of ‘Test’ [$F(1, 17) = 6.569, p = 0.020, \text{partial } \eta^2 = 0.279$]. Post-hoc t-tests showed that the functional connectivity between the left TPJ and the left OFA increased from post-test to pre-test measurement [$t(8) = 3.914, p = 0.005, \text{Cohen's } d = 1.305$]. There was no significant change in the healthy control group [$t(9) = 0.619, p = 0.551$].

Moreover, we used the left FFA as the target region and measured the functional connectivity change associated with the left FFA. We found that the functional connectivity between the left and right FFA changed with training, as shown in Figure 24B. A two-way mixed-design ANOVA showed that there was a significant interaction between the ‘Group’ and the ‘Test’ factor [$F(1, 17) = 18.75, p = 0.0005, \text{partial } \eta^2 = 0.524$]. Post-hoc t-tests showed that there was a significant decrease in the functional connectivity between the left and right FFA [$t(8) = 4.221, p = 0.003, \text{Cohen's } d = 1.407$].

Moreover, there was a significant increase in the functional connectivity between the left and right FFA [$t(9) = 2.698$, $p = 0.025$, Cohen's $d = 0.853$].

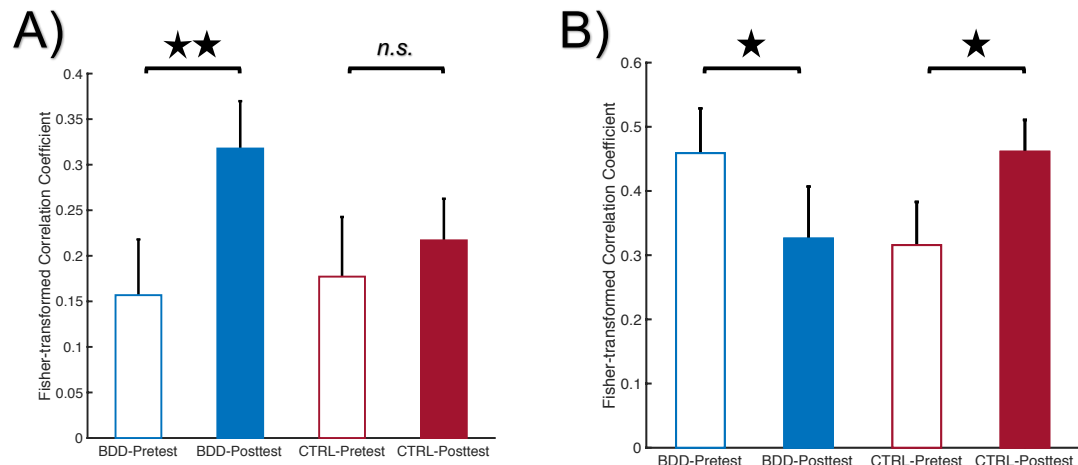


Figure 24. Functional connectivity change. A) Fisher-transformed correlation coefficient between the left TPJ and the right OFA. There was a significant increase in the correlation coefficient in the BDD group after training. B) Fisher-transformed correlation coefficient between the left and right FFA. There was a significant decrease in bilateral connectivity in the FFA for the BDD group. There was significant increase in bilateral connectivity in the FFA for the healthy control group. ** $p < .01$. * $p < .05$.

Discussion and Conclusion

In Experiment 6, we trained BDD subjects and healthy control subjects on detecting LSF faces over the course of 6 sessions. Both groups showed improvements in detecting LSF faces. Consistent with our hypothesis, we found a substantial decrease of BOLD activities in the left TPJ and a significant increase of right dominance in the FFA for the BDD group. Moreover, we found a significant change of functional connectivity in association with the left TPJ and the FFAs, suggesting a global change in both the ventral and dorsal pathways of face processing for the BDD group after VPL. Moreover,

the healthy control subjects decreased their right dominance in FFA in the ventral pathway after VPL.

Our study has several important implications. Our results indicated that training low spatial frequency face stimuli could induce global changes in the face processing pathways where low spatial frequency information is processed. Similar to the VPL studies using simple visual stimuli and primitive visual features, we provided further evidence that feature-based learning and plasticity are associated with representation change in the brain, regardless of the stimuli' complexity (Watanabe & Sasaki, 2015).

Second, we showed that feature-based learning could enhance behavioral performance and induce BOLD changes in patients with deficits that originated from higher-level visual areas. BDD patients showed deficits in association with holistic visual processing, in particular left dominance in brain activities and imbalance between the featural and holistic processing. After learning low spatial frequency visual features, the BDD patients showed behavioral improvement and manifested corresponding BOLD activities changes that correlated with the behavioral improvement. Moreover, by training low spatial frequency faces that feature holistic processing, there was an increase in right dominance of FFA, which is characteristic of holistic processing. Additionally, there was a decrease in the activity in TPJ, which is characteristic of emotional and featural processing. These results demonstrated that feature-based learning can influence BDD patients' holistic processing in a targeted manner and may be developed as a promising clinical tool as an intervention for the patient population.

Third, our results demonstrated a substantially different mechanism of learning between the BDD and healthy control subjects. We propose that the improvement of

holistic processing in BDD patients has been associated with a transition from the dorsal processing pathway to the ventral processing pathway. Previous studies have suggested an imbalance between the featural and holistic processing, namely a hyperactivation of featural processing and a lack of activation in the holistic processing, underlies the abnormalities of BDD patients. After a training procedure featuring holistic processing, the activity in the TPJ decreased, manifesting a lower activation in the dorsal featural processing pathway. Meanwhile, the FFA activity becomes right dominant, namely, similar to the normal BOLD activity in healthy control subjects. Therefore, the BOLD activity transits from more featural processing to more holistic processing. Functional connectivity changes also accompanied the BOLD activity transition. We speculated that the increase in functional connectivity between TPJ and OFA might suggest that the processing of low spatial frequency faces transited from dorsal to ventral through the increased connection between TPJ and the OFA, which is the input to the ventral processing pathway. On the other hand, we propose that an increased left FFA activity drove the improvement in healthy control subjects. This result is consistent with previous studies (Bi et al., 2014; Rossion et al., 2000) investigating the learning of face views in which the left FFA activity also increased after training. We propose that the left FFA is more plastic in healthy control subjects compared to the right FFA. The reason might be that the right FFA is over-specialized and over-developed for face processing in healthy adult subjects, and therefore there is more room for improvement in the left FFA.

The functional connectivity changes in the FFA and the BOLD activity change in the FFA lateralization index might suggest a mechanism underlying FFA dominance. Initially, BDD patients showed left dominance with higher functional connectivity

between the left and right FFA. The healthy control subjects showed right dominance with lower functional connectivity between the left and right FFA. After training, the increase in right dominance of BDD patients was accompanied by lower functional connectivity. In contrast, the decreased right dominance of healthy control subjects was accompanied by higher functional connectivity between the two FFAs. Therefore, the dominance of the right FFA might result from less connectivity between the two hemispheres. Nevertheless, more studies are necessary to clarify the relationship between functional connectivity and dominance.

One potential argument that may undermine the current study is the controversy underlying the processing of low spatial frequency faces. While most studies support the processing of low frequency faces as holistic processing in the FFA and the ventral pathway, some studies suggested that low spatial frequency faces were also processed in the dorsal pathway (Rotshtein et al., 2007; Vuilleumier et al., 2003). However, depending on different tasks, presentation times, and subjects' attention to different visual features, the processing of low frequency faces involves different brain areas. In Experiment 6, the presentation time is short and might involve the ventral processing pathway to a larger extent.

It is not entirely clear whether task-based plasticity occurred or not with Experiment 6. Although we observed a dissociation between the healthy control subjects and BDD patients, since task-relevant learning is involved, it is challenging to exclude task-based plasticity. One possibility is that task-based plasticity occurred at the initial stage of learning, and at a later stage, feature-based plasticity occurred. One future direction of Experiment 6 is to train low spatial frequency faces with task-irrelevant

learning or neurofeedback to isolate the effects of feature-based plasticity in association with complex visual features.

Another future direction of Experiment 6 is to evaluate the symptoms and cognitive biases of BDD patients. In Experiment 6, we focused on the behavior and BOLD activity change in association with feature-based learning.

To conclude, Aim 3 showed that feature-based learning of faces involves changes in the face representation areas. Moreover, VPL of faces induced global changes in the BDD patients and may be used as a potential intervention for BDD patients.

General Discussion and Conclusions

Visual perceptual learning refers to the long-term performance improvement with visual experiences. Visual perceptual learning provides an insight into how learning and plasticity develop in general in the brain. One of the controversies in visual perceptual learning is how the brain learns visual features. The dissertation focuses on the discussion of feature-based visual learning in three aims.

Aim 1 and Aim 2 addresses how feature-based learning is developed with primitive visual features using simple visual stimuli. A two-stage model has summarized the learning of simple visual features as feature-based plasticity, which involves a feature-representation change in the brain.

Aim 1 addresses which brain areas are associated with feature-based plasticity using decoded fMRI neurofeedback. We repetitively induced the brain activation pattern corresponding to a Sekuler display in early visual areas V1/V2. The Sekuler display, if presented visually, induces the perception of the local motion directions and a global motion direction which is the temporal and spatial average of the local motion directions. Local motions were processed in V1/V2, whereas global motion was processed in V3A and beyond. By inducing the brain activation pattern corresponding to the Sekuler display, subjects improved on discriminating the motion directions that corresponded to the local motion ranges but not specifically to the global motion direction. Therefore, we concluded that feature-based plasticity is induced with representation change in early visual areas.

Aim 2 addresses what factors are involved in the development of feature-based plasticity. Specifically, we focused on how reward and arousal can evoke visual perceptual learning. We presented rewards either before or after the visual stimulus in different groups. Reward presented before the visual stimulus did not evoke learning. Reward presented after the visual stimulus induced visual learning for the orientation paired with the water reward. Moreover, there was no transfer to the untrained orientation or the untrained eye. Arousal played a different role in learning. Arousal sound presented before the visual stimulus and after the visual stimulus can both induce learning in the orientation paired with the sound. Moreover, arousal presented before the visual stimulus induced the learning to transfer to the untrained orientation. Furthermore, arousal presented after the visual stimulus induced the learning to transfer to the untrained orientation and location.

We quantified the effects of reward and arousal with the normalization model. The psychophysical data were best fitted by modeling the arousal as an excitatory effect and modeling the reward as an inhibitory effect.

In Aim 3, we addressed how feature-based learning is developed with natural and socially relevant visual stimuli with complex visual features. We trained BDD patients and healthy control subjects with low spatial frequency face stimuli. Previous studies suggested a dissociation between the processing pathway of low spatial frequency face stimuli. In BDD patients, the low spatial frequency faces were processed in both the ventral and dorsal pathways of the brain. On the contrary, the healthy control subjects processed the low spatial frequency faces only in the ventral pathway of the brain. After training with low spatial frequency faces, the BDD patients showed changes in both the

ventral and dorsal processing pathways. On the other hand, the healthy control subjects only showed changes in the dorsal processing pathway. The dissociation suggested that training of complex visual stimuli will induce changes in association with the representation of features in the brain.

The current dissertation's future direction is to investigate the neural mechanisms of how reward and arousal induce feature-based learning. Moreover, the BDD patients and healthy control subjects also dissociate in high spatial frequency processing. Another future direction is to train both subject groups with high spatial frequency processing to explore whether they dissociate when processing high spatial frequency features.

To conclude, the learning of visual features is related to the representation change in the brain. It is also strongly influenced by the reward and arousal levels associated with delivering the visual stimulus.

References

- Ahissar, M., & Hochstein, S. (1997). Task difficulty and the specificity of perceptual learning. In (Vol. 387, pp. 401-406).
- Ahissar, M., & Hochstein, S. (2004). The reverse hierarchy theory of visual perceptual learning. *Trends in cognitive sciences*, 8(10), 457-464. doi:10.1016/j.tics.2004.08.011
- Arienzo, D., Leow, A., Brown, J. A., Zhan, L., Gadelkarim, J., Hovav, S., & Feusner, J. D. (2013). Abnormal brain network organization in body dysmorphic disorder. *Neuropsychopharmacology*, 38(6), 1130-1139. doi:10.1038/npp.2013.18
- Arsenault, J. T., & Vanduffel, W. (2019). Ventral midbrain stimulation induces perceptual learning and cortical plasticity in primates. *Nat Commun*, 10(1), 3591. doi:10.1038/s41467-019-11527-9
- Astle, A. T., Blighe, A. J., Webb, B. S., & McGraw, P. V. (2015). The effect of normal aging and age-related macular degeneration on perceptual learning. *J Vis*, 15(10), 16. doi:2473637 [pii] 10.1167/15.10.16 [doi]
- Aston-Jones, G., & Cohen, J. D. (2005). AN INTEGRATIVE THEORY OF LOCUS COERULEUS-NOREPINEPHRINE FUNCTION: Adaptive Gain and Optimal Performance. *Annual review of neuroscience*, 28(1), 403-450. doi:10.1146/annurev.neuro.28.061604.135709
- Beilharz, F., Castle, D. J., Grace, S., & Rossell, S. L. (2017). A systematic review of visual processing and associated treatments in body dysmorphic disorder. *Acta Psychiatr Scand*, 136(1), 16-36. doi:10.1111/acps.12705

- Bi, T., Chen, J., Zhou, T., He, Y., & Fang, F. (2014). Function and structure of human left fusiform cortex are closely associated with perceptual learning of faces. *Curr Biol*, 24(2), 222-227. doi:10.1016/j.cub.2013.12.028
- Bijleveld, E., Custers, R., & Aarts, H. (2009). The Unconscious Eye Opener: Pupil Dilation Reveals Strategic Recruitment of Resources Upon Presentation of Subliminal Reward Cues. *Psychological Science*, 20(11), 1313-1315. doi:10.1111/j.1467-9280.2009.02443.x
- Braddick, O. J., O'Brien, J. M., Wattam-Bell, J., Atkinson, J., Hartley, T., & Turner, R. (2001). Brain areas sensitive to coherent visual motion. *Perception*, 30(1), 61-72. doi:10.1068/p3048
- Brainard, D. H. (1997). The Psychophysics Toolbox. *Spat Vis*, 10(4), 433-436.
- Bruns, P., & Watanabe, T. (2019). Perceptual learning of task-irrelevant features depends on the sensory context. *Sci Rep*, 9(1), 1666. doi:10.1038/s41598-019-38586-8
- Carandini, M., & Heeger, D. J. (2011). Normalization as a canonical neural computation. *Nat Rev Neurosci*, 13(1), 51-62. doi:10.1038/nrn3136
- Doshier, B., & Lu, Z.-L. (2017). Visual Perceptual Learning and Models. *Annual Review of Vision Science*, 3(1), 343-363. doi:10.1146/annurev-vision-102016-061249
- Duchaine, B., & Yovel, G. (2015). A Revised Neural Framework for Face Processing. *Annu Rev Vis Sci*, 1, 393-416. doi:10.1146/annurev-vision-082114-035518
- Engel, S. A., Rumelhart, D. E., Wandell, B. A., Lee, A. T., Glover, G. H., Chichilnisky, E. J., & Shadlen, M. N. (1994). fMRI of human visual cortex. *Nature*, 369(6481), 525. doi:10.1038/369525a0 [doi]

Feusner, J. D., Moller, H., Altstein, L., Sugar, C., Bookheimer, S., Yoon, J., & Hembacher, E. (2010). Inverted face processing in body dysmorphic disorder. *J Psychiatr Res*, *44*(15), 1088-1094. doi:10.1016/j.jpsychires.2010.03.015

Feusner, J. D., Moody, T., Hembacher, E., Townsend, J., McKinley, M., Moller, H., & Bookheimer, S. (2010). Abnormalities of visual processing and frontostriatal systems in body dysmorphic disorder. *Arch Gen Psychiatry*, *67*(2), 197-205. doi:10.1001/archgenpsychiatry.2009.190

Feusner, J. D., Townsend, J., Bystritsky, A., & Bookheimer, S. (2007). Visual information processing of faces in body dysmorphic disorder. *Arch Gen Psychiatry*, *64*(12), 1417-1425. doi:64/12/1417 [pii] 10.1001/archpsyc.64.12.1417 [doi]

Fischl, B. (2012). FreeSurfer. *Neuroimage*, *62*(2), 774-781. doi:S1053-8119(12)00038-9 [pii] 10.1016/j.neuroimage.2012.01.021 [doi]

Fize, D., Vanduffel, W., Nelissen, K., Denys, K., Chef d'Hotel, C., Fugeras, O., & Orban, G. A. (2003). The retinotopic organization of primate dorsal V4 and surrounding areas: A functional magnetic resonance imaging study in awake monkeys. *J Neurosci*, *23*(19), 7395-7406. doi:23/19/7395 [pii]

Frank, S. M., Qi, A., Ravasio, D., Sasaki, Y., Rosen, E. L., & Watanabe, T. (2020). Supervised Learning Occurs in Visual Perceptual Learning of Complex Natural Images. *Curr Biol*, *30*(15), 2995-3000 e2993. doi:S0960-9822(20)30737-5 [pii] 10.1016/j.cub.2020.05.050 [doi]

- Frankó, E., Seitz, A. R., & Vogels, R. (2010). Dissociable Neural Effects of Long-term Stimulus–Reward Pairing in Macaque Visual Cortex. *Journal of Cognitive Neuroscience*, 22(7), 1425-1439. doi:10.1162/jocn.2009.21288
- Galliusi, J., Grzeczowski, L., Gerbino, W., Herzog, M. H., & Bernardis, P. (2018). Is lack of attention necessary for task-irrelevant perceptual learning? *Vision Res*, 152, 118-125. doi:10.1016/j.visres.2017.10.006
- Glasser, M. F., Coalson, T. S., Robinson, E. C., Hacker, C. D., Harwell, J., Yacoub, E., . . . Van Essen, D. C. (2016). A multi-modal parcellation of human cerebral cortex. *Nature*, 536(7615), 171-178. doi:10.1038/nature18933
- Goffaux, V., Peters, J., Haubrechts, J., Schiltz, C., Jansma, B., & Goebel, R. (2011). From coarse to fine? Spatial and temporal dynamics of cortical face processing. *Cereb Cortex*, 21(2), 467-476. doi:10.1093/cercor/bhq112
- Grill-Spector, K., Knouf, N., & Kanwisher, N. (2004). The fusiform face area subserves face perception, not generic within-category identification. *Nat Neurosci*, 7(5), 555-562. doi:10.1038/nn1224
- Gutnisky, D. A., Hansen, B. J., Iliescu, B. F., & Dragoi, V. (2009). Attention alters visual plasticity during exposure-based learning. *Curr Biol*, 19(7), 555-560. doi:10.1016/j.cub.2009.01.063
- Harris, A., & Aguirre, G. K. (2008). The representation of parts and wholes in face-selective cortex. *J Cogn Neurosci*, 20(5), 863-878. doi:10.1162/jocn.2008.20509 [doi]
- Harris, A., & Aguirre, G. K. (2010). Neural tuning for face wholes and parts in human fusiform gyrus revealed by fMRI adaptation. *J Neurophysiol*, 104(1), 336-345. doi:jn.00626.2009 [pii]

10.1152/jn.00626.2009 [doi]

Harris, H., Glikberg, M., & Sagi, D. (2012). Generalized perceptual learning in the absence of sensory adaptation. *Current Biology*, 22(19), 1813-1817.

doi:10.1016/j.cub.2012.07.059

Haxby, J. V., & Gobbini, M. I. (2011). *Distributed neural systems for face perception*: The Oxford Handbook of Face Perception.

Hensch, T. K. (2005a). Critical period mechanisms in developing visual cortex. *Curr Top Dev Biol*, 69, 215-237. doi:10.1016/s0070-2153(05)69008-4

Hensch, T. K. (2005b). Critical period plasticity in local cortical circuits. *Nat Rev Neurosci*, 6(11), 877-888. doi:10.1038/nrn1787

James, W. (1890). The perception of reality. *Principles of psychology*, 2, 283-324.

Jeter, P. E., Doshier, B. A., Liu, S. H., & Lu, Z. L. (2010). Specificity of perceptual learning increases with increased training. *Vision Research*, 50(19), 1928-1940.

doi:10.1016/j.visres.2010.06.016

Kahnt, T., Grueschow, M., Speck, O., & Haynes, J. D. (2011). Perceptual learning and decision-making in human medial frontal cortex. *Neuron*, 70(3), 549-559.

doi:10.1016/j.neuron.2011.02.054

Kanwisher, N., McDermott, J., & Chun, M. M. (1997). The fusiform face area: a module in human extrastriate cortex specialized for face perception. *Journal of neuroscience*, 17(11), 4302-4311.

Kanwisher, N., & Yovel, G. (2006). The fusiform face area: a cortical region specialized for the perception of faces. *Philos Trans R Soc Lond B Biol Sci*, 361(1476), 2109-2128.

doi:10.1098/rstb.2006.1934

- Karni, A., & Sagi, D. (1991). Where practice makes perfect in texture discrimination: evidence for primary visual cortex plasticity. *Proceedings of the National Academy of Sciences*, 88, 4966-4970.
- Karni, A., & Sagi, D. (1993). The time course of learning a visual skill. *Nature*, 365(6443), 250-252. doi:10.1038/365250a0
- Kerwin, L., Hovav, S., Hellemann, G., & Feusner, J. D. (2014). Impairment in local and global processing and set-shifting in body dysmorphic disorder. *J Psychiatr Res*, 57, 41-50. doi:10.1016/j.jpsychires.2014.06.003
- Kim, D., Lokey, S., & Ling, S. (2017). Elevated arousal levels enhance contrast perception. *Journal of Vision*, 17(2), 14-14. doi:10.1167/17.2.14
- Koyama, S., Sasaki, Y., Andersen, G. J., Tootell, R. B. H., Matsuura, M., & Watanabe, T. (2005). Separate Processing of Different Global-Motion Structures in Visual Cortex Is Revealed by fMRI. *Current Biology*, 15(22), 2027-2032.
doi:<https://doi.org/10.1016/j.cub.2005.10.069>
- Law, C.-T., & Gold, J. I. (2008). Neural correlates of perceptual learning in a sensory-motor, but not a sensory, cortical area. *Nature neuroscience*, 11, 505-513.
doi:10.1038/nn2070
- Law, C.-T., & Gold, J. I. (2009). Reinforcement learning can account for associative and perceptual learning on a visual-decision task. *Nature neuroscience*, 12, 655-663.
doi:10.1038/nn.2304
- Leuchs, L., Schneider, M., Czisch, M., & Spormaker, V. I. (2017). Neural correlates of pupil dilation during human fear learning. *Neuroimage*, 147, 186-197.
doi:10.1016/j.neuroimage.2016.11.072

Levi, D. M. (2012). Prentice Award Lecture 2011: Removing the Brakes on Plasticity in the Amblyopic Brain. *Optometry and Vision Science*, 89(6), 827-838.

doi:10.1097/OPX.0b013e318257a187

Li, W., Arienzo, D., & Feusner, J. D. (2013). Body Dysmorphic Disorder: Neurobiological Features and an Updated Model. *Z Klin Psychol Psychother (Gott)*, 42(3), 184-191. doi:10.1026/1616-3443/a000213

Lorenzino, M., & Caudek, C. (2015). Task-irrelevant emotion facilitates face discrimination learning. *Vision Res*, 108, 56-66. doi:10.1016/j.visres.2015.01.007

Maniglia, M., Pavan, A., Sato, G., Contemori, G., Montemurro, S., Battaglini, L., & Casco, C. (2016). Perceptual learning leads to long lasting visual improvement in patients with central vision loss. *Restor Neurol Neurosci*, 34(5), 697-720. doi:RNN150575 [pii] 10.3233/RNN-150575 [doi]

Maniglia, M., Soler, V., & Trotter, Y. (2020). Combining fixation and lateral masking training enhances perceptual learning effects in patients with macular degeneration. *J Vis*, 20(10), 19. doi:2770929 [pii] 10.1167/jov.20.10.19 [doi]

McGinley, M. J. (2020). Brain States: Sensory Modulations All the Way Down. *Curr Biol*, 30(20), R1263-R1266. doi:10.1016/j.cub.2020.07.094

Miyawaki, Y., Uchida, H., Yamashita, O., Sato, M. A., Morito, Y., Tanabe, H. C., . . .

Kamitani, Y. (2008). Visual image reconstruction from human brain activity using a combination of multiscale local image decoders. *Neuron*, 60(5), 915-929.

doi:10.1016/j.neuron.2008.11.004

- Moody, T. D., Sasaki, M. A., Bohon, C., Strober, M. A., Bookheimer, S. Y., Sheen, C. L., & Feusner, J. D. (2015). Functional connectivity for face processing in individuals with body dysmorphic disorder and anorexia nervosa. *Psychol Med, 45*(16), 3491-3503. doi:10.1017/S0033291715001397
- Öner, M., & Deveci Kocakoç, İ. (2017). Jmasm 49: A compilation of some popular goodness of fit tests for normal distribution: Their algorithms and matlab codes (matlab). *Journal of Modern Applied Statistical Methods, 16*(2), 30.
- Pascucci, D., Mastropasqua, T., & Turatto, M. (2015). Monetary reward modulates task-irrelevant perceptual learning for invisible stimuli. *PLoS One, 10*(5), e0124009. doi:10.1371/journal.pone.0124009
- Pavlovskaya, M., & Hochstein, S. (2011). Perceptual learning transfer between hemispheres and tasks for easy and hard feature search conditions. *Journal of Vision, 11*(1), 8-8. doi:10.1167/11.1.8.Introduction
- Phillipou, A., & Castle, D. (2015). Body dysmorphic disorder in men. *Aust Fam Physician, 44*(11), 798-801.
- Phillips, K. A. (2009). *Understanding body dysmorphic disorder*: Oxford University Press.
- Plank, T., Rosengarth, K., Schmalhofer, C., Goldhacker, M., Brandl-Ruhle, S., & Greenlee, M. W. (2014). Perceptual learning in patients with macular degeneration. *Front Psychol, 5*, 1189. doi:10.3389/fpsyg.2014.01189 [doi]
- Polat, U. (2009). Making perceptual learning practical to improve visual functions. *Vision Res, 49*(21), 2566-2573. doi:S0042-6989(09)00282-X [pii] 10.1016/j.visres.2009.06.005 [doi]

- Polat, U., Ma-Naim, T., Belkin, M., & Sagi, D. (2004). Improving vision in adult amblyopia by perceptual learning. *Proc Natl Acad Sci U S A*, *101*(17), 6692-6697. doi:10.1073/pnas.0401200101 [doi] 0401200101 [pii]
- Polat, U., Ma-Naim, T., & Spierer, A. (2009). Treatment of children with amblyopia by perceptual learning. *Vision Res*, *49*(21), 2599-2603. doi:S0042-6989(09)00330-7 [pii] 10.1016/j.visres.2009.07.008 [doi]
- Posner, M. I., & Petersen, S. E. The attention system of the human brain. (0147-006X (Print)).
- Protopapas, A., Mitsi, A., Koustoumbardis, M., Tsitsopoulou, S. M., Leventi, M., & Seitz, A. R. (2017). Incidental orthographic learning during a color detection task. *Cognition*, *166*, 251-271. doi:10.1016/j.cognition.2017.05.030
- Rescorla, R. A., & Wagner, A. R. (1972). A theory of Pavlovian conditioning: Variations in the effectiveness of reinforcement and nonreinforcement. *Classical Conditioning II Current Research and Theory*, *21*(6), 64-99. doi:10.1101/gr.110528.110
- Reynolds, J. H., & Heeger, D. J. (2009). The normalization model of attention. *Neuron*, *61*(2), 168-185. doi:10.1016/j.neuron.2009.01.002
- Richler, J. J., & Gauthier, I. (2014). A meta-analysis and review of holistic face processing. *Psychol Bull*, *140*(5), 1281-1302. doi:10.1037/a0037004
- Roelfsema, P. R., van Ooyen, A., & Watanabe, T. (2010). Perceptual learning rules based on reinforcers and attention. *Trends in Cognitive Sciences*, *14*, 64-71. doi:10.1016/j.tics.2009.11.005

Rosa, A. M., Silva, M. F., Ferreira, S., Murta, J., & Castelo-Branco, M. (2013). Plasticity in the human visual cortex: An ophthalmology-based perspective. *BioMed Research International*, 2013.

Rosenthal, O., & Humphreys, G. W. (2010). Perceptual organization without perception. The subliminal learning of global contour. *Psychol Sci*, 21(12), 1751-1758.
doi:10.1177/0956797610389188

Rossion, B., Gauthier, I., Tarr, M. J., Despland, P., Bruyer, R., Linotte, S., & Crommelinck, M. (2000). The N170 occipito-temporal component is delayed and enhanced to inverted faces but not to inverted objects: an electrophysiological account of face-specific processes in the human brain. *Neuroreport*, 11(1), 69-72.

Rotshtein, P., Vuilleumier, P., Winston, J., Driver, J., & Dolan, R. (2007). Distinct and convergent visual processing of high and low spatial frequency information in faces. *Cereb Cortex*, 17(11), 2713-2724. doi:10.1093/cercor/bhl180

Sagi, D. (2011). Perceptual learning in Vision Research. *Vision Research*, 51(13), 1552-1566. doi:<https://doi.org/10.1016/j.visres.2010.10.019>

Salzman, C. D., Murasugi, C. M., Britten, K. H., & Newsome, W. T. (1992). Microstimulation in visual area MT: effects on direction discrimination performance. *J Neurosci*, 12(6), 2331-2355. doi:10.1523/jneurosci.12-06-02331.1992

Samson, D., Apperly, I. A., Chiavarino, C., & Humphreys, G. W. (2004). Left temporoparietal junction is necessary for representing someone else's belief. *Nat Neurosci*, 7(5), 499-500. doi:10.1038/nn1223

- Sara, S. J., & Bouret, S. (2012). Orienting and Reorienting: The Locus Coeruleus Mediates Cognition through Arousal. *Neuron*, *76*(1), 130-141.
doi:10.1016/j.neuron.2012.09.011
- Sasaki, Y., Nanez, J. E., & Watanabe, T. (2010). Advances in visual perceptual learning and plasticity. *Nature reviews. Neuroscience*, *11*(1), 53-60. doi:10.1038/nrn2737
- Saxe, R., & Kanwisher, N. (2003). People thinking about thinking people: The role of the temporo-parietal junction in “theory of mind”. *Neuroimage*, *19*(4), 1835-1842.
doi:10.1016/s1053-8119(03)00230-1
- Schiltz, C., & Rossion, B. (2006). Faces are represented holistically in the human occipito-temporal cortex. *Neuroimage*, *32*(3), 1385-1394. doi:S1053-8119(06)00568-4
[pii]
10.1016/j.neuroimage.2006.05.037 [doi]
- Schoups, A. (2001). Practising orientation identification improves orientation coding in V1 neurons. *412*, 5.
- Schultz, W. (2002). Getting formal with dopamine and reward. *Neuron*, *36*, 241-263.
doi:10.1016/S0896-6273(02)00967-4
- Schultz, W. (2006). Behavioral Theories and the Neurophysiology of Reward. *Annual Review of Psychology*, *57*, 87-115. doi:10.1146/annurev.psych.56.091103.070229
- Schultz, W. (2015). Neuronal Reward and Decision Signals: From Theories to Data. *Physiological Reviews*, *95*(3), 853-951. doi:10.1152/physrev.00023.2014
- Schultz, W. (2016). Dopamine reward prediction-error signalling: a two-component response. *Nature Reviews Neuroscience*, *17*(3), 183-195. doi:10.1038/nrn.2015.26

- Schultz, W., Dayan, P., & Montague, P. R. (1997). A Neural Substrate of Prediction and Reward. *Science*, 275(5306), 1593-1599. doi:10.1126/science.275.5306.1593
- Seitz, A. R., & Dinse, H. R. (2007). A common framework for perceptual learning. *Current Opinion in Neurobiology*, 17(2), 148-153.
doi:<https://doi.org/10.1016/j.conb.2007.02.004>
- Seitz, A. R., Kim, D., & Watanabe, T. (2009). Rewards Evoke Learning of Unconsciously Processed Visual Stimuli in Adult Humans. *Neuron*, 61, 700-707.
doi:10.1016/j.neuron.2009.01.016
- Seitz, A. R., & Watanabe, T. (2003). Psychophysics: Is subliminal learning really passive? *Nature*, 422(6927), 36-36. doi:10.1038/422036a
- Shibata, K., Lisi, G., Cortese, A., Watanabe, T., Sasaki, Y., & Kawato, M. (2019). Toward a comprehensive understanding of the neural mechanisms of decoded neurofeedback. *Neuroimage*, 188, 539-556. doi:10.1016/j.neuroimage.2018.12.022
- Shibata, K., Sagi, D., & Watanabe, T. (2014). Two-stage model in perceptual learning: toward a unified theory. *Annals of the New York Academy of Sciences*, 1316, 18-28.
doi:10.1111/nyas.12419
- Shibata, K., Sasaki, Y., Bang, J. W., Walsh, E. G., Machizawa, M. G., Tamaki, M., . . . Watanabe, T. (2017). Overlearning hyperstabilizes a skill by rapidly making neurochemical processing inhibitory-dominant. *Nature neuroscience*, 20(3), 470-475.
doi:10.1038/nn.4490
- Shibata, K., Watanabe, T., Sasaki, Y., & Kawato, M. (2011). Perceptual Learning Incepted by Decoded fMRI Neurofeedback Without Stimulus Presentation. *Science*, 334(6061), 1413-1415. doi:10.1126/science.1212003

- Sterkin, A., Levy, Y., Pokroy, R., Lev, M., Levian, L., Doron, R., . . . Polat, U. (2018). Vision improvement in pilots with presbyopia following perceptual learning. *Vision Res*, *152*, 61-73. doi:S0042-6989(17)30205-5 [pii]
10.1016/j.visres.2017.09.003 [doi]
- Toda, A., Imamizu, H., Kawato, M., & Sato, M. A. (2011). Reconstruction of two-dimensional movement trajectories from selected magnetoencephalography cortical currents by combined sparse Bayesian methods. *Neuroimage*, *54*(2), 892-905. doi:S1053-8119(10)01257-7 [pii]
10.1016/j.neuroimage.2010.09.057 [doi]
- Tsuchiya, N., & Koch, C. (2004). Continuous flash suppression reduces negative afterimages. *Nature neuroscience*(1097-6256 (Print)).
- Tsushima, Y., Seitz, A. R., & Watanabe, T. (2008). Task-irrelevant learning occurs only when the irrelevant feature is weak. *Current Biology*, *18*(12), 516-517.
doi:10.1016/j.cub.2008.04.029
- Vinck, M., Batista-Brito, R., Knoblich, U., & Cardin, J. A. (2015). Arousal and locomotion make distinct contributions to cortical activity patterns and visual encoding. *Neuron*, *86*(3), 740-754. doi:10.1016/j.neuron.2015.03.028
- Vuilleumier, P., Armony, J. L., Driver, J., & Dolan, R. J. (2003). Distinct spatial frequency sensitivities for processing faces and emotional expressions. *Nature neuroscience*, *6*(6), 624-631.
- Wang, R., Cong, L.-J., & Yu, C. (2013). The classical TDT perceptual learning is mostly temporal learning. *Journal of Vision*, *13*(5), 9-9. doi:10.1167/13.5.9.doi

- Wang, R., Zhang, J.-y., Klein, S. A., Levi, D. M., & Yu, C. (2012). Task relevancy and demand modulate double-training enabled transfer of perceptual learning. *Vision Research*, *61*, 33-38. doi:10.1016/j.visres.2011.07.019
- Wang, Z., Kim, D., Pedroncelli, G., Sasaki, Y., & Watanabe, T. (2019). Reward Evokes Visual Perceptual Learning Following Reinforcement Learning Rules. *bioRxiv*, 760017. doi:10.1101/760017
- Watanabe, T., Náñez, J. E., Koyama, S., Mukai, I., Liederman, J., & Sasaki, Y. (2002). Greater plasticity in lower-level than higher-level visual motion processing in a passive perceptual learning task. *Nature neuroscience*, *5*(10), 1003-1009. doi:10.1038/nn915
- Watanabe, T., Nanez, J. E., & Sasaki, Y. (2001). Perceptual learning without perception. *Nature*, *413*(6858), 844-848.
- Watanabe, T., & Sasaki, Y. (2015). Perceptual Learning: Toward a Comprehensive Theory. *Annual review of psychology*(August), 1-25. doi:10.1146/annurev-psych-010814-015214
- Watanabe, T., Sasaki, Y., Shibata, K., & Kawato, M. (2017). Advances in fMRI Real-Time Neurofeedback. *Trends in Cognitive Sciences*, *21*(12), 997-1010. doi:10.1016/j.tics.2017.09.010
- Williams, D. F., & Sekuler, R. (1984). Coherent global motion percepts from stochastic local motions. *Vision Research*, *24*(1)(0042-6989 (Print)), 55-62.
- Xiao, L.-Q., Zhang, J.-Y., Wang, R., Klein, S. a., Levi, D. M., & Yu, C. (2008). Complete transfer of perceptual learning across retinal locations enabled by double training. *Current biology : CB*, *18*(24), 1922-1926. doi:10.1016/j.cub.2008.10.030

- Xue, X., Zhou, X., & Li, S. (2015). Unconscious reward facilitates motion perceptual learning. *Visual Cognition*, 23(1-2), 161-178. doi:10.1080/13506285.2014.981625
- y Cajal, S. R. (2004). *Advice for a young investigator*: Mit Press.
- Yamashita, O., Sato, M. A., Yoshioka, T., Tong, F., & Kamitani, Y. (2008). Sparse estimation automatically selects voxels relevant for the decoding of fMRI activity patterns. *Neuroimage*, 42(4), 1414-1429. doi:S1053-8119(08)00694-0 [pii] 10.1016/j.neuroimage.2008.05.050 [doi]
- Yotsumoto, Y., Chang, L.-H., Ni, R., Pierce, R., Andersen, G. J., Watanabe, T., & Sasaki, Y. (2014). White matter in the older brain is more plastic than in the younger brain. *Nature Communications*, 5, 5504-5504. doi:10.1038/ncomms6504
- Yotsumoto, Y., Chang, L. H., Watanabe, T., & Sasaki, Y. (2009). Interference and feature specificity in visual perceptual learning. *Vision Research*, 49(21), 2611-2623. doi:10.1016/j.visres.2009.08.001
- Yotsumoto, Y., Sasaki, Y., Chan, P., Vasios, C. E., Bonmassar, G., Ito, N., . . . Watanabe, T. (2009). Location-Specific Cortical Activation Changes during Sleep after Training for Perceptual Learning. *Current Biology*, 19(15), 1278-1282. doi:10.1016/j.cub.2009.06.011
- Yotsumoto, Y., Watanabe, T., & Sasaki, Y. (2008). Different Dynamics of Performance and Brain Activation in the Time Course of Perceptual Learning. *Neuron*, 57(6), 827-833. doi:10.1016/j.neuron.2008.02.034
- Yovel, G. (2016). Neural and cognitive face-selective markers: An integrative review. *Neuropsychologia*, 83, 5-13. doi:10.1016/j.neuropsychologia.2015.09.026

Yu, Q., Zhang, P., Qiu, J., & Fang, F. (2016). Perceptual Learning of Contrast Detection in the Human Lateral Geniculate Nucleus. *Current Biology*, *26*(23), 3176-3182.

doi:10.1016/j.cub.2016.09.034

Zhang, J.-Y., Kuai, S.-G., Xiao, L.-Q., Klein, S. a., Levi, D. M., & Yu, C. (2008).

Stimulus Coding Rules for Perceptual Learning. *PLoS Biology*, *6*(8), e197-e197.

doi:10.1371/journal.pbio.0060197

Zhang, J.-Y., Zhang, G.-L., Xiao, L.-Q., Klein, S. a., Levi, D. M., & Yu, C. (2010). Rule-based learning explains visual perceptual learning and its specificity and transfer. *The Journal of neuroscience : the official journal of the Society for Neuroscience*, *30*(37),

12323-12328. doi:10.1523/JNEUROSCI.0704-10.2010

Zhang, T., Xiao, L.-Q., Klein, S. a., Levi, D. M., & Yu, C. (2010). Decoupling location specificity from perceptual learning of orientation discrimination. *Vision Research*, *50*(4),

368-374. doi:10.1016/j.visres.2009.08.024